UNIVERSITY OF PADUA

Department of Land, Environment, Agriculture and Forestry

Mediterranean Forestry and Natural Resource Management

Mapping Fire Regimes in China Using MODIS Data

Supervisor

Dr. Francesco Pirotti

Co-Supervisor

Prof. José M.C. Pereira

Dongmei Chen

No. 1089793

Academic Year

2014 – 2015

CONTENTS

List of figures

List of tables

Abbreviations and acronyms

CV	inter-annual Coefficient of Variance
CVAB	inter-annual Coefficient of Variation in annual Area Burned
CVNF	inter-annual Coefficient of Variation in annual Number of Fires
DOY	day of year
FRP	fire radiative power
FSD	fire season duration
FPM	Fire pixels in Peak Month
HCF	High annual and peak month area burned, Cropland and Forest
LC	land cover
LCG	Low annual and peak month area burned, Cropland and Grassland
LFS	Low annual and peak month area burned, Forest and Savanna
MAAB	mean annual area burned
MANF	mean annual number of fires
MODIS	Moderate Resolution Imaging Spectroradiometer
NA	not available
PC	principal component
PCA	principal component analysis

Abstract

Relatively little is known about the vegetation fire regimes in China. To investigate the fire regime characteristics and the potential drivers, twelve fire regime variables were selected and computed in grid cells cover: (1) fire frequency and its inter-annual variability, (2) annual burned area and its inter-annual variability, (3) frequency-size inequality, (4) seasonality, (5) fire intensity and (6) land cover types affected by fires, using MODIS burned area and active fire data during 2001 to 2014. The variables were normalized and the principal components were extracted and clustered.

The results showed that approximately 67.9% of land in China is affected by wildfires, and around 3.3% burned area is with relatively high fire activity located mainly in Northeast and East China. The barren or sparsely vegetated western China is nearly fire free. Active fires were detected in Central China but the area burned was not detectable from MODIS. Forest fires in northern China are relatively large, less frequent, with a short fire season peaks in non-winter seasons and higher inter-annual variability, implying that there is a higher probability of lightning fires. In contrast, forest fires in southern China are relatively small, more frequent, with a long fire season peaks in non-summer seasons and lower inter-annual variability, implying that they were mostly caused by anthropogenic ignitions. Low inter-annual variability and low intensity were associated with cropland fires, whereas grassland fires more likely exhibit the opposite. Four fire regimes were discriminated on the basis of data sources, burned area and vegetation types.

The distribution of fire characteristics is driven by a combination of fuel, topography, climate and human activities. The proposed fire regimes could help to identify the ecological role of fire, and to support fire risk mitigation and natural resources management decisions. Further research is needed to have a more comprehensive understanding of fire regimes in China.

Keywords

Fire regimes, remote sensing, MODIS, cluster analysis, fire drivers, China.

1. Introduction

Since late Silurian period (~ 420 million years ago), fire has played a role modifying the atmosphere and influencing ecosystem structure and function in Earth history (Summers *et al.*, 2011). Fire acts as a prominent disturbance factor and an agent of environmental change significantly impacting terrestrial, aquatic, and atmospheric systems throughout the world (Lentile *et al.*, 2006; Roy *et al.*, 2013). Fires are local events, with regional scale characteristics, governed by global scale climate patterns (Summers *et al.*, 2011). They are the main responsible of atmospheric pollution in tropical latitudes, the principal agent of deforestation and land use change in the rain forest, and one of the most prominent sources of land degradation in Mediterranean areas of Europe (Chuvieco, 2000). They also influence germination and plant regeneration thus controlling species succession and structure and their evolutionary fire-prone traits in ecosystems (Moreno & Chuvieco, 2013; Barros & Pereira, 2014).

To better understand the role of fire, the concept of fire regime was introduced to describe the spatial and temporal fire characteristics in terms of fire occurrence, spread, behavior and effects, such as fire frequency, seasonality of fires, fire intensity and severity and the types and patterns of fires. Fire regimes result from dynamic and complex processes controlled by the interactions and feedbacks between fire, climate, vegetation attributes, landscape characteristics, land use and ignition patterns (Barros & Pereira, 2014) and tend to change along with the alterations of these factors, which vary in multiple temporal and spatial scales. However, the pattern and extent of constraint associated with fire characteristics can be predicted. For example, fire intensity is strongly determined by the amount of fuel available, whereas frequency and fire seasonality might be more closely related to the probability of flammable conditions; furthermore, fire frequency should be negatively related to maximum fireline intensity since when fire is frequent, fuel load is more difficult to accumulate for producing high-intensity fires (Archibald *et al.*, 2013).

Fire regimes are important to evaluate the effects of fire, and to predict how patterns of fire might change in response to environmental and human drivers (Archibald *et al.*, 2013), further, to assist in fire risk mitigation and natural resources management for managers and policy-makers. For instance, fire effects could be mild or positive with long history of fire regimes because vegetation and soils are typically adapted to fire conditions, or potentially negative if fire regimes change rapidly even become intense and frequent (Moreno & Chuvieco, 2013).

The study of fire regimes has been prolifically and widely carried out in various spatial and temporal scales, covering topics, for example, from how plant species adapt to wildfire (Fernandes & Rigolot, 2007), to how landscape interacts with wildfire (Moreira *et al.*, 2011); from characterizing wildfire regimes in decades (Malamud *et al.*, 2005), to discussing fire regimes in millenniums (Gill *et al.*, 2009); from reconstructing the incidence of past fire and its relationship to changing climate and vegetation (Gavin *et al.*, 2007), to monitoring the occurrence of fires responding to the change of climate and vegetation currently (Pausas, 2004). The influence of climate change and anthropogenic activity in altering the past, current and future fire regimes has become a dominant research topic in recent fire regime study (Guyette *et al.*, 2002; Gillett *et al.*, 2004; Marlon *et al.*, 2008; Bowman *et al.*, 2009).

In China, fire regimes were predominantly investigated in a local scale in Northeast China. Interesting case studies are the spatial patterns and the possible drivers of fire occurrence and how it responses to climate change in a boreal forest (Liu *et al.*, 2012), the long-term effects of fire suppression on a forest landscape in the Great Xing'an Mountains change fire regimes in this region (Chang *et al.*, 2007; Wang *et al.*, 2007), and the development of customized fire behavior fuel models for boreal forests of northeastern China (Wu *et al.*, 2011). Relatively scarce literature can be found on the characterization of wildfire regimes in China. Krawchuk and Moritz (2009) modelled the spatial distribution of fire regimes in China by quantifying the relationship between LANDFIRE fire regime classes and a global climate data set in comparison with the United States. However, a direct measurement of fire regimes at national scale in China is still missing and it is very important to fill this gap to understand the

ecological role of wildfires.

It is worthy to notice that field data are typically absent or deficient, as in China, where data sources from satellites coupled with simulation models are often used in forest fires detection, burning emission estimation, and forest fire risks (Zhang *et al.*, 2011). Hence, the use of remote sensing can play an indispensable role in characterizing fire regimes globally and locally. Chuvieco *et al.* (2008) defined global fire regimes by developing a set of metrics representing three axes of fire activity: fire density, seasonal duration and inter-annual variability from Moderate Resolution Imaging Spectroradiometer (MODIS) active fire data. Archibald *et al.* (2013) also identified five key characteristics of fire regimes globally: size, frequency, intensity, season, and extent, using a combined dataset including MODIS data and Global Fire Emissions Database (GFED). However, to the extent of our knowledge, similar studies have not been carried out at a national/local scale using global remotely sensed estimates of active fire and burned area, and we believe that local scale study can provide different perspectives on remotely sensed fire regimes from a global scale one.

China is a mountainous country with the world's largest population density. The lifted Tibetan Plateau together with a geographic difference that the eastern margin is connected with ocean but the western boundary abuts the large Eurasian landmass has formed an "east wet, west dry" bioclimatic pattern. Human activity is the dominant cause of fires although the possibility of fire occurrences may vary greatly with climate, vegetation and landscape, nevertheless, the fire regimes in China are still poorly understood as far as we know.

In this study, our research objectives are to characterize fire regimes in China deriving from MODIS burned area and active fire data and further discuss the interactions between fires and dominant drivers of fire regimes (climate, vegetation and landscape) as well as the potential influences of anthropogenic factors on the fire regimes, with implications for fire risks mitigation and natural resources (vegetation and land) management.

2. Review of Literature

Fire regime as a key concept in disturbance ecology at present has not been clearly and strictly defined, yet being widely used in many scientific areas. It is also quite a difficult concept to be defined in practice, considering the complex biophysical environment in multiple spatial extent and timescales and anthropogenic factors (Krebs *et al.*, 2010). Krebs *et al.* (2010) have reviewed at length how the concept of fire regime originated from French had evolved and spread in English literatures especially after the release of the Leopold Report, when the idea of fire disturbance in ecosystems was introduced and adopted. The paper presented the used definitions of fire regimes on factors reflecting ignition conditions, burning process and fire effects in various temporal and spatial scales. Also, they proposed drawing different types of definitions of fire regime according to the study objectives and the level of complexity. Similarly, Conedera *et al.* (2009) suggested defining fire regime flexibly combing user-defined fire attributes and the physical nature of fire under its biological context.

Furthermore, they both differentiated fire regimes in a strict sense ("sensu stricto"), which assembles the core components describing which fire (type, intensity, fire behavior, etc.), when (frequency, seasonality, synchronicity, etc.) and where (size, shape of fires, etc.) it occurs, and a wide sense ("sensu lato"), which clusters conditions controlling fire occurrence (fuel characteristics, fire weather, anthropogenic conditions, etc.), immediate fire effects (severity, mortality, costs and damages, etc.), and derived or composite parameters resulting from the combination of two or more basic variables and conceived to represent some complex characteristics of fire occurrence (trends, variations, classifications systems, etc.) (Conedera *et al.*, 2009; Krebs *et al.*, 2010). Davies (2013) also claimed fire intensity, fire frequency, fire extent and fire effect are the four key components in fire regime concept. In addition, the concept of fire regime is recommended to be examined across multiple temporal and spatial scales to characteristic the nature of fire within a biome integrating all possible variations in climate, fuel properties, and human influences in a paleoecological

perspective (Whitlock *et al.*, 2010).

Therefore, fire regime refers to the nature of fires occurring over an extended period of time, and it can be spatially described by a particular combination of fire characteristics, e.g. frequency, size, intensity, seasonality, severity, or combined descriptors (Morgan *et al.*, 2001; Archibald *et al.*, 2013). The frequency of fire can be measured as the average number of fires that burn over a given area per unit time, or the number of times that fires occur within a defined area and time period, and in a relatively small landscape area it can be expressed as fire rotation period, fire cycle, fire return interval, or probability of occurrence. Fire frequency is mostly controlled by fuel accumulation, moisture availability, ignition sources and human activities (Morgan *et al.*, 2001; Summers *et al.*, 2011; Davies, 2013). The magnitude of fire behavior and effects is described as fire intensity, a measure of fire behavior relating to the rate of heat release, and fire severity, the physical impacts of the fire directly associated with combustion and heat transfer (Davies, 2013). The seasonality of vegetation fires is driven by climate factors, ignition sources, and land use management practices (Benali *et al.*, 2013). Those fire regime descriptors vary according to the spatial or temporal scale at which they are measured (Morgan *et al.*, 2001), and the data availability also limits the way how they are measured.

Mapping fire regime provides decision supports on fire risk assessment and control, ecosystem restoration and natural resource management, and helps to quantify fire emissions and indentify knowledge gaps (Morgan *et al.*, 2001; Archibald *et al.*, 2013; Gundy & Melissa, 2014).

Various data resources from fire history records (Kasischke & Turetsky, 2006; Moreno & Chuvieco, 2013; Mansuy *et al.*, 2014), fire atlases (Rollins *et al.*, 2001; Holden *et al.*, 2005; Shapiro-Miller *et al.*, 2007), fire scars (Fulé *et al.*, 2003; Guyette *et al.*, 2005; Falk *et al.*, 2011), and satellite data (Oliveira *et al.*, 2012; Archibald *et al.*, 2013; Molinario *et al.*, 2014) are used in assessing fire regime, particularly remote sensed data is of great assistance in identifying fire regimes globally or in regional studies where field-based data is absent. Researchers have also made efforts to search supports from studies on paleoecology (Flannigan *et al.*, 2001; Lynch *et al.*,

2004), chemistry and climatology (Guyette *et al.*, 2012), and other indirect evidences (Krawchuk & Moritz, 2009; Gundy & Melissa, 2014). Since those data resources have their own strengths and weaknesses in utility of describing different aspects in fire regimes, a combination of different types of data often helps to overcome the limitations of individual data sets and supplement the data deficiency (Morgan *et al.*, 2001; Holden *et al.*, 2005; Shapiro-Miller *et al.*, 2007; Krawchuk & Moritz, 2009). However, in the global scale of fire regime study, only remotely sensed data are able to capture the fire characteristics, despite the temporal scale is not satisfied to define the historical role of fires and there are uncertainties in accuracy assessment of the data products (Chuvieco *et al.*, 2008; Archibald *et al.*, 2013).

Although the approaches used in mapping fire regime are dynamic due to the study scales and data availability, the trend of applying integrated methods (e.g. combined data sets, remote sending and Geographic Information Systems (GIS), simulation and modeling) and multi-scale analysis in investigating the interactions among wildfires, vegetation, landscape, climate and human activities has become more evident (Rollins *et al.*, 2004; Falk *et al.*, 2007; Rollins, 2009; Falk *et al.*, 2011). Recently researchers also tend to be more interested in studying the changes of fire regime under climate change and socioeconomic developments (Kasischke & Turetsky, 2006; Pausas & Fernández-Muñoz, 2012; Pezzatti *et al.*, 2013; Moreno *et al.*, 2014; Fréjaville & Curt, 2015).

The study of wildfire in China has been concentrating on forest fires, particularly in northeastern China after the catastrophic 1987 forest fires in this region. Many studies focused on the influence factors from natural (e.g. climate change, insect outbreak) and human disturbance (e.g. reforestation, fire suppression) on fire regime (Wang *et al.*, 2006; Wang *et al.*, 2007; Chen *et al.*, 2011; Liu *et al.*, 2012), or the impact of fire on the forest production and landscape in this area, mostly by using LANDIS simulation model (Wang *et al.*, 2001; Li *et al.*, 2013). According to their studies, fire occurrence density in northern China is positively related to the degree of temperature and precipitation change, fire frequency would be reduced by larch caterpillar disturbances and high fire suppression, while fire intensity would be

decreased by larch caterpillar disturbances but increased by high fire suppression. Those factors would also influence the fire regime by changing the structure of fuel types, for example, both high fire suppression and reforestation would increase larch, but decrease white birch, however, larch caterpillar disturbances have the opposite impacts (Wang *et al.*, 2007; Chen *et al.*, 2011). The effects of human actions may have a stronger influence on fire occurrence than climate change (Liu *et al.*, 2012). Fire exclusion can lead to catastrophic fires with return intervals ranging from 50 to 120 years, increase the proportion of coniferous forests and decrease the proportion of deciduous forests, simplify tree species composition, and alter forest age structures and landscape patterns (Chang *et al.*, 2007).

Remote sensing and simulation models have been widely used in detecting forest fire hot spots, predicting fire risks and quantifying fire emissions in China (Calle *et al.*, 2005; Yan *et al.*, 2006; Zhang *et al.*, 2011; Huang *et al.*, 2012; He *et al.*, 2013; Tian *et al.*, 2013), which are the main fire research topics in China. Fire regime, however, is with relatively little literature, especially a national scale. The distribution characteristics of forest fires and change of forest fire dynamic in China was studied and the results both showed that forest fires were mainly distributed in the south and southwest regions of China and mostly occurred in spring, caused by prescribed burning and agricultural fires (Tian *et al.*, 2013; Tian *et al.*, 2014). Nevertheless, fire regimes in China were firstly indirectly predicted and defined in LANDFIRE classification from statistical comparison with the United States based on the ecological similarities between the two land masses (Krawchuk & Moritz, 2009). They proposed a very high probability of grass fires with a 0 to 35 years return interval largely in Northeast and East China, shrub fires with a 35 to 200 years return interval in West China, where barren lands are the predominant land cover type at present, and forest fires with a 0 to 35 years return interval in a small area in Southwest China. On the contrary, absent fire activity in South and Southeast China was predicted in their study.

3. Methodology

Figure 1 shows the overall workflow of the methods developed for this thesis.

3.1 Satellite data collection

MODIS is a remote sensing instrument on board the morning-descending Terra (launched 1999) and afternoon-descending Aqua (launched 2002) polar-orbiting NASA satellites, with a revisit cycle of 1 to 2 days, including bands specifically designed for fire detection (Roy *et al.*, 2013; Oliveras *et al.*, 2014). The MODIS standard burned area product (MCD64A1) produced by the University of Maryland was collected from ftp://fuoco.geog.umd.edu/db/MCD64A1/. The MODIS standard active fire data (Global Monthly Fire Location Product - MCD14ML) and the MODIS land cover type product (Land Cover Dynamics Yearly - MCD12Q1) were both downloaded from https://earthdata.nasa.gov/.

The detection of burned areas, i.e. areas affected by fire within a certain time interval, is based on the effects of fire on vegetation, such as structural change of vegetation, charcoal on the ground and exposed soil, using the MODIS algorithm locating the occurrence of rapid changes in daily surface reflectance (Roy *et al.*, 2005). The MCD64A1 is a monthly product generated from applying the active-fire based burned area mapping algorithm on the 500-m MODIS cloud-free surface reflectance imagery (Giglio *et al.*, 2009). It contains burn dates in ordinal day as a burning information layer in Hierarchical Data Format (HDF). The MODIS tiles of approximately 10 degrees x 10 degrees in size, assigned a horizontal (h) and vertical (v) coordinate (spatial extent) and ordered by Julian date of the starting day of the month (temporal scale), were merged to create a monthly map of the approximate study area by using GDAL in raster format. Then the monthly burn date maps from 2001 to 2014 were used in further data processing. A mask of the Chinese boundaries was applied to select the region of interest.

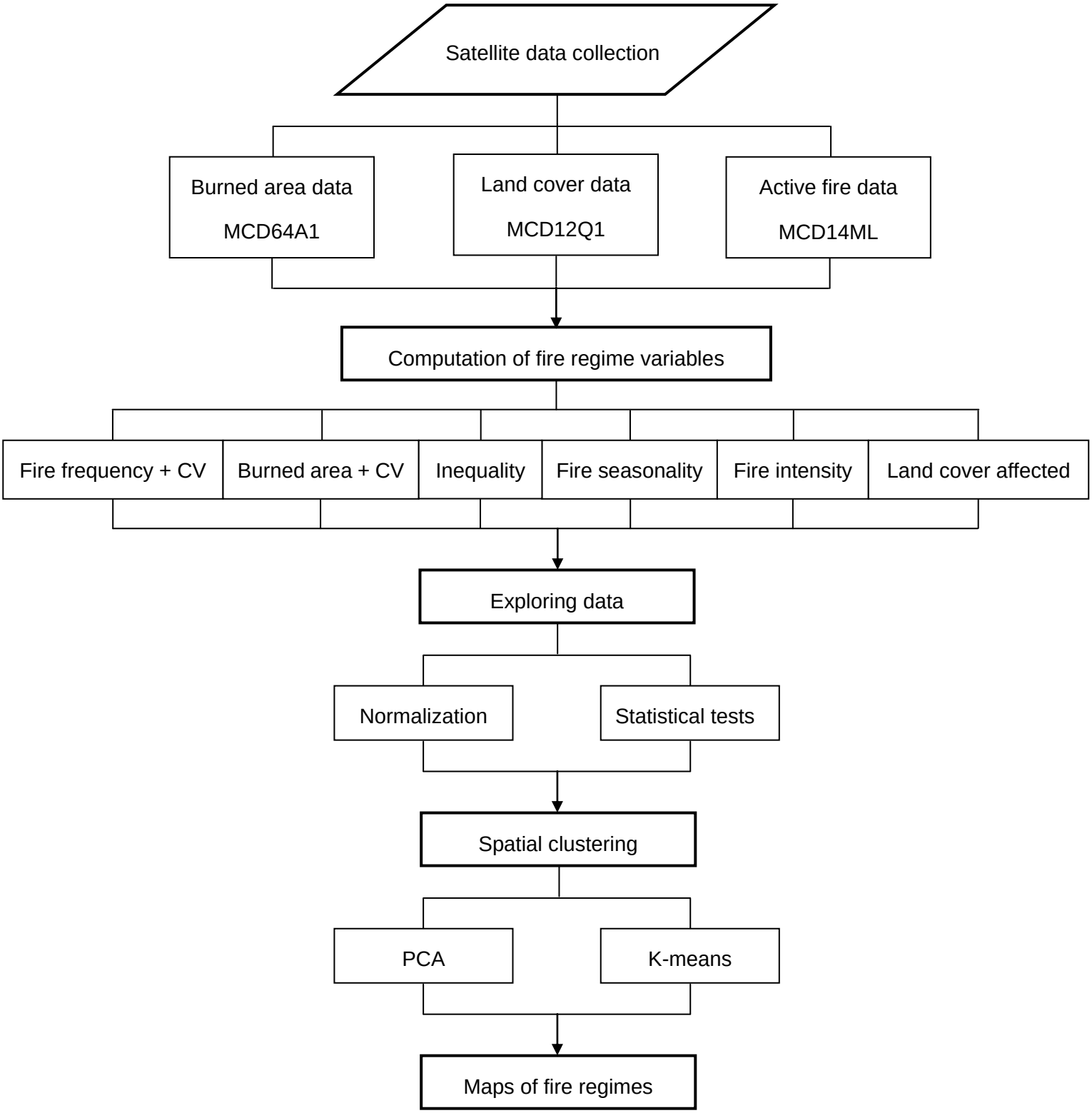

Figure 1 Flowchart of methods

The detection of active fires, i.e. fires actively burning at the overpass time of the satellite under relatively cloud-free conditions, is mostly based on temperature using a contextual algorithm (Giglio *et al.*, 2003). The MCD14ML was collected year by year by using NASA firms archive download tool in a shape file data point format at 1km resolution, and was then converted to raster data format from point selecting fire radiative power value field and setting cell size at 0.0045 degree and same raster in pixels with burned area data in ArcGIS. Each point of fire radiative power in the map was counted as a fire pixel in the computation.

The MCD12Q1 is a yearly product at 500m × 500m spatial resolution contains five global land cover classification systems, in which the IGBP (International Geosphere-Biosphere Programme) global vegetation classification scheme was chosen in this study. The tiles were merged to create a yearly map of land cover in China from 2001 to 2012. The 16 land cover classes from the scheme were then aggregated into the four land cover classes in this study, i.e. forests, savannas, grasslands and croplands, as following: (1) the land cover classes enumerated from 1 to 5, which describing different types of forests were grouped in the forests class; (2) the land cover classes enumerated from 6 to 9, which including shrublands and savannas, were grouped in savannas class for the reasons that very few fire pixels were detected in shrub lands and the marked similarity between shrubland and savanna; (3) the land cover class 10 was retained as grasslands class; (4) the land cover class 12 and 14 were grouped to croplands class, and (5) the rest non-vegetation land cover classes including wetlands, urban and built-up, snow and ice, barren or sparsely vegetated were all set as no data value to be excluded in the analysis of vegetation fires.

3.2 Study area

This study is on fire regime in the whole China located in East Asia, between 17.5°N and 54°N latitude and 73°E and 135.7°E longitude and with an area about 960 million km^2 and a population of 1.3 billion.

According to the remote sensed images of land cover in this study, around 75% of China land covered with vegetation types, mainly forest, savanna, grassland and cropland, and shrublands only take up 2% area of the five vegetation types. The forest area especially in northeastern and central China has been increasing as observed in the land cover maps during periods available (2001 - 2012) in MODIS land cover product (see Figure 2). This was primarily because of large-scale afforestation efforts in China. China's forests represent 34% of Asia's forests and 5% of the worlds' forests, around 207 million ha, which cover 22% of China land area (He *et al.*, 2011).

The forests are mostly distributed in Great Xing'an Mountains, Xiao Xing'an Mountains, and Changbai Mountains in northeastern regions, Qin Mountains and Hengduan Mountains in southwestern regions and other regions in southern China. The plains in Northeast and North China and Sichuan basin in Southwest China are largely occupied for agricultural uses. The Inner Mongolia Plateau, Tibetan Plateau and Huangtu Plateau are widely covered with grasslands and the area around the Yunnan-Guizhou plateau is mixed with savannas and grassland. In contrast, the other western part of China is sparsely vegetated or barren, where only Altai Mountains and Tianshan are visibly vegetated.

The climate in China is diversified due to its wide span of latitude and mountainous topography, and the location of land and ocean. The Tibetan Plateau has significant influence on China climate, which has formed a unique plateau cold climate in the Southwest, and greatly impacted the monsoon climate in the East and the arid climate in the Northwest coupled with atmospheric circulation. The eastern part of China mostly has a monsoon climate, with hot, humid summers and cold, dry winters. Arid climate impacted by westerlies is prevailing in the northwestern inland regions, where deserts or barren lands are the typical landscape.

As the most populous country in the world, China has experienced evident environmental degradation under intensive human activities in many regions. The consequential change of landscape and climate, accompany with the direct impact of human activities, also plays a very important role in fire regime in China. The development of urbanization has shifted a large part of population from rural areas to

metropolises, leading to a remarkable decreasing of agricultural manpower and the consequent accumulation of fuel load in fields. Given slash-and-burn cultivation and crop residue burning are traditional agricultural practices especially in southwestern China, agricultural fires occur regularly in those farm lands.

a)

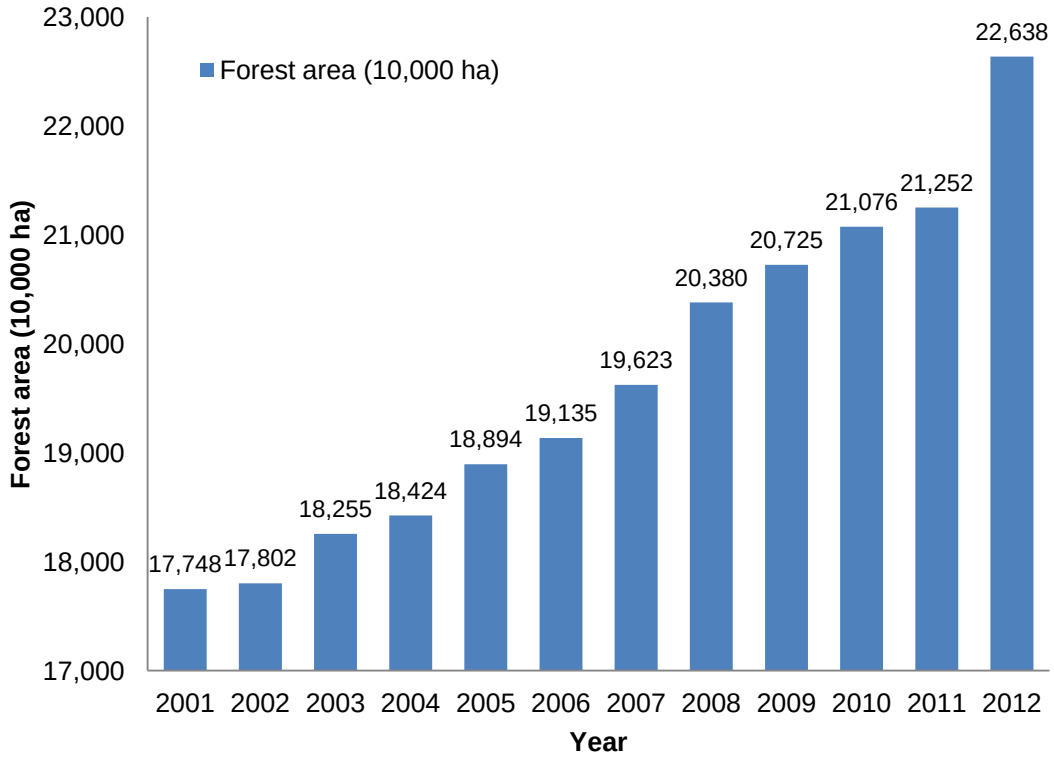

b)

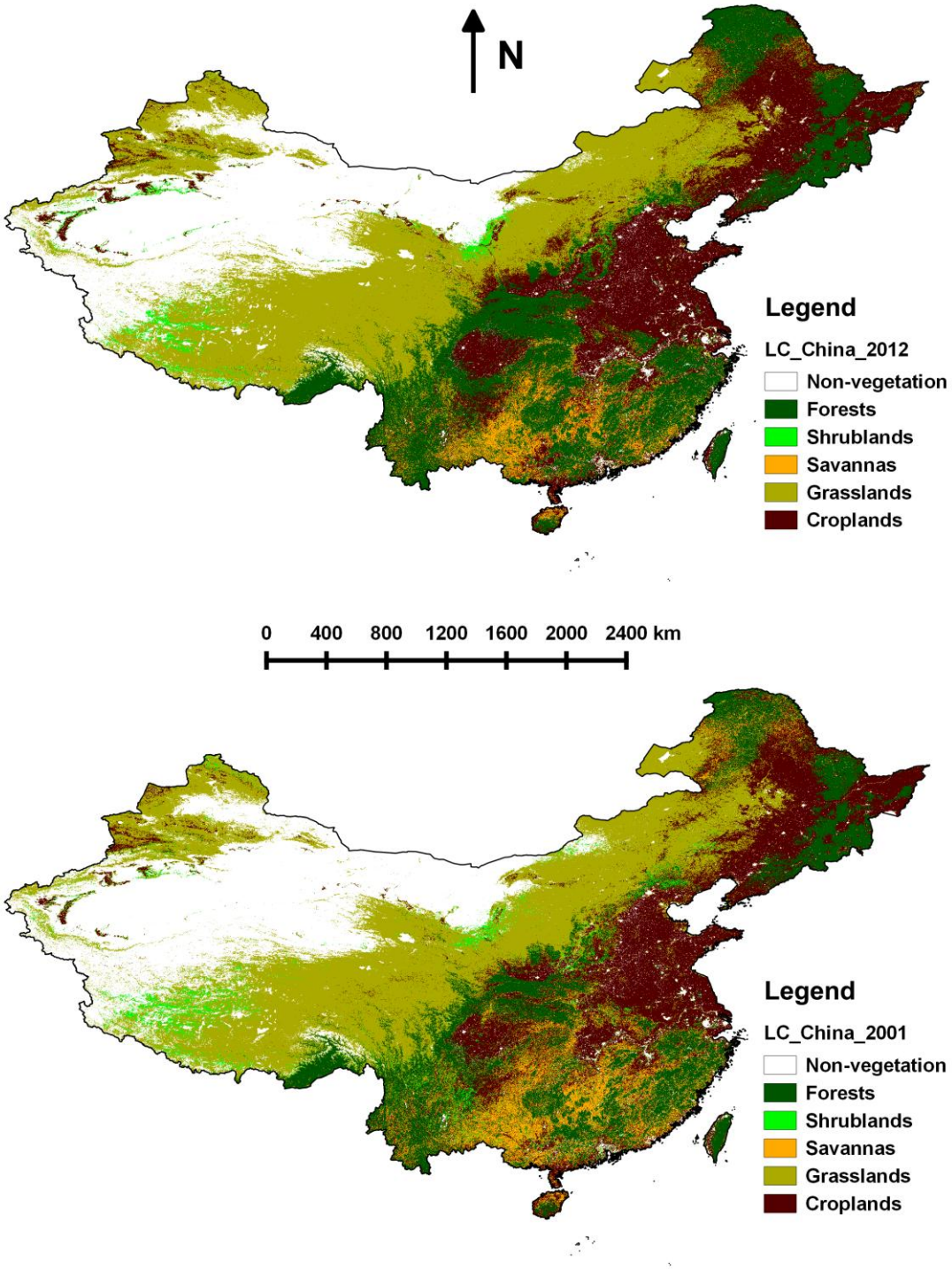

Figure 2 Yearly forest area calculated (a) and land cover of China in 2001 and 2012 observed (b) from MODIS

3.3 Computation of fire regime variables

We computed twelve variables to characterize the fire regimes in China by using available remotely sensed data. The variables were chosen to describe the spatial, temporal and intensity attributes of fire regime. Specifically, these are: (1) mean annual number of fires; (2) inter-annual coefficient of variance in annual number of fires; (3) mean annual area burned; (4) inter-annual coefficient of variance in annual area burned; (5) Gini index of fire sizes; (6) 90^{th} percentile of fire radiative power; (7) fire season duration; (8) fire pixels in peak month; (9) percentage of forests affected by fire; (10) percentage of savannas affected by fire; (11) percentage of grasslands affected by fire; and (12) percentage of croplands affected by fire. All the twelve variables were calculated in 0.5 degree grid cells using MATLAB and the output were further mapped in QGIS. A detailed description of the considered variables is provided in the following.

3.3.1 Mean annual number of fires (MANF, fires·yr^{-1})

The modified flood-fill algorithm was applied to identify individual fires in burned area maps (Archibald & Roy, 2009). The algorithm is initialized by randomly picking one burnt pixel that is inserted in a list L of pixels to be examined. A first burnt pixel set as centre pixel is given fireID of 1 then those eight neighbouring pixels recorded within 8 days of the centre pixel are given identical fireID. Furthermore, they are inserted in a list L of spatial positions to be examined, while the current centre pixel is deleted from L. Then, if L is not empty, recursively one of the pixels in L is considered as centre pixels and the algorithm executes the same operations described above. If L is empty, then a new burnt pixel (not previously considered) is randomly picked as centre pixels among the available ones, the value of fireID is increased by1, and the algorithm repeats the usual operations for the centre pixels as described above. This procedure ends when all the burnt pixels have been considered. Count all unique non-zero fireID in all years to calculate the number of fires in each grid cell of every 100×100 pixels.

In each grid cell, the mean annual number of fires is:

$$\mathrm{MANF} = \frac{\sum_1^{\mathrm{y}} \sum_1^{\mathrm{m}} \mathrm{F}_{\mathrm{y,m}}}{\mathrm{y} \times \mathrm{m}}$$

where y is the number of years and m is the number of months in one year, F is the number of fires detected by the modified flood-fill algorithm from MCD64A1 monthly maps during the month m in year y. Fire frequency in this study refers to mean annual number of fires per grid cell.

3.3.2 Inter-annual coefficient of variation in annual number of fires (CVNF)

The inter-annual coefficient of variation in number of fires is defined as the ratio of the standard deviation of annual number of fires and the mean annual number of fires.

In each grid cell, the inter-annual coefficient of variation in number of fires is:

$$\mathrm{CVNF} = \frac{\sqrt{\frac{1}{\mathrm{y}-1} \sum_1^{\mathrm{y}} \left|\mathrm{F}_{\mathrm{y}} - \mathrm{MANF}\right|^2}}{\mathrm{MANF}}$$

where F is the annual number of fires detected in year y by summing up the number of fires from monthly burned area maps.

3.3.3 Mean annual area burned (MAAB, $km^2 \cdot yr^{-1}$)

Every pixel with a burn date in a grid cell is counted during all years, then the number of these pixels times 0.25 returns the annual area burned in the grid cell in a unit of square kilometers, and the function is as following:

$$\mathrm{MAAB} = \frac{\sum_1^{\mathrm{y}} \sum_1^{\mathrm{m}} \mathrm{P}_{\mathrm{y,m}} \times 0.25}{\mathrm{y} \times \mathrm{m}}$$

where P is the number of fire pixels detected during month m in year y.

3.3.4 Inter-annual coefficient of variation in annual area burned (CVAB)

The inter-annual coefficient of variation in area burned is defined as the ratio of the standard deviation of annual area burned and the mean annual area burned.

In each grid cell, the inter-annual coefficient of variation in area burned is:

$$\mathrm{CVAB} = \frac{\sqrt{\frac{1}{\mathrm{y}-1} \sum_1^{\mathrm{y}} \left|\left(\mathrm{P}_{\mathrm{y}} \times 0.25\right) - \mathrm{MAAB}\right|^2}}{\mathrm{MAAB}}$$

where P is the total number of fire pixels detected in year y.

3.3.5 Gini index of fire sizes

Gini index of fire sizes is introduced to characterize the inequality in fire size distributions, i.e. to what extent area burned at a given location tends to concentrate

on a small number of larger fires, or is distributed through a large number of relatively smaller fires. The higher Gini index indicates the larger burned area occurred in less times of burning.

Gini index can be computed following the steps to calculate the Gini Index with the Lorenz derivation (Bellù & Liberati, 2006). The function is as following:

$$G = 1 - \sum_{i} [(q_i + q_{i-1})(p_i - p_{i-1})]$$

where q_i is the cumulative proportion of burned area and p_i is the cumulative proportion of times fires occurred.

3.3.6 Fire radiative power (FRP, mW/m^2)

Fire radiative power data is directly retrieved from active fire data. The 90th percentile of fire radiative power value, which was reported as a reasonable predictor of burn severity (Heward *et al.*, 2013), and probably provides the best information of fireline intensity in distinguishing systems that have the potential to burn at very high intensities from those in which there is insufficient fuel to result in high-intensity fires (Archibald *et al.*, 2013), is chosen to discriminate fire regimes.

3.3.7 Fire season duration in days (FSD)

Fire season duration is defined as the number of days from when 10 % of fire pixels were seen in a grid cell to when 90% of the fire pixels were detected (Innes *et al.*, 2000).

3.3.8 Fire pixels in peak month (FPM)

The peak month in burned area is the month when the maximum fire pixels occurred in one month decided by comparing accumulated fire pixels in each month during the 14 years.

3.3.9 Percentage of land cover types affected by fires

Percentage of land cover types, i.e. forests, savannas, grasslands, croplands, affected by fires is calculated as the ratio of fire pixels in each land cover type and the total fire pixels in the grid cell.

3.4 Exploratory factor analysis of fire regime variables

To check sampling adequacy of factor analysis, the cell grids along all the twelve variables were included in a Kaiser–Meyer–Olkin (KMO) measure (Kaiser & Rice, 1974) in R. The range of KMO is from 0 to 1 and a value higher 0.5 is desired. A Fligner-Killeen test, which is believed most robust against departures from normality for homogeneity of variance (Conover *et al.*, 1981) was performed after the examination of normality in all variables. The null hypothesis in Fligner-Killeen test is that variances in all variables are equal; the alternative hypothesis is that at least two of them differ. The *p*-value of Fligner-Killeen test should be significant.

The extraction of principal components followed by building a correlation matrix containing the principal directions in variables was done in MATLAB to explore the structure of standardized variables data and understand the impact factors in the further cluster analysis.

3.5 Cluster analysis of fire regimes

Before the clustering algorithm was applied, the fire regime variables were normalized by mean and standard deviation. To acquire a better understanding on clusters, the cluster analysis was performed with principal components as input data. The number of principal components was decided by the percentage of variability explained by fire regime variables is at least 80%. K-means algorithm was chosen to cluster the fire characteristics because different cluster algorithms have provided similar results and k-means is simpler.

The appropriate number of clusters was determined by comparing the sum of squared error (SSE) for a number of cluster solutions in R. SSE, which can be seen as a global measure of error, is defined as the sum of the squared distance between each member of a cluster and its cluster centroid. Thus, an appropriate number of clusters could be defined as the number at which the reduction in SSE slows dramatically (“elbow”). The significance of the components in each cluster is tested from a one-way Multivariate Analysis of Variance (MANOVA) in MATLAB.

4. Results

5141 grid cells are included in the study area but only 3493 grid cells have fire records combing active fire counts (3440 grid cells) and burned pixels (2218 grid cells), indicating that more than two thirds of China land is affected by wild fires based on MODIS active fire and burned area data.

4.1 Fire regime variables

4.1.1 Fire frequency and its inter-annual variability

The MANF distribution shows that the most fire-prone areas are located mainly in East-central China, especially in the boundary among the four eastern provinces (Henan, Shandong, Anhui and Jiangsu), and Northeast China in Heilongjiang, followed by Southwest China in Yunan and Guizhou, and South China in Guangdong, then few areas in West China in Xinjiang. Higher fire frequency is observed in the East, South, and most west of China, but in the western and central part of China most of the land is fire-free based on burned area data (Figure 3 a).

Low inter-annual coefficient of variation in annual number of fires has been observed in the areas where high fire frequency detected, while in the regions where fire events occurred casually the stability of fire frequency is very weak, and those regions are located mainly in Northeast China in Inner Mongolia, Liaoning and Jilin, central-western regions and few areas in southeastern China. Overall, the inter-annual variability of fire frequency in most of southern, eastern and northeastern China is relatively low (Figure 3 b).

a)

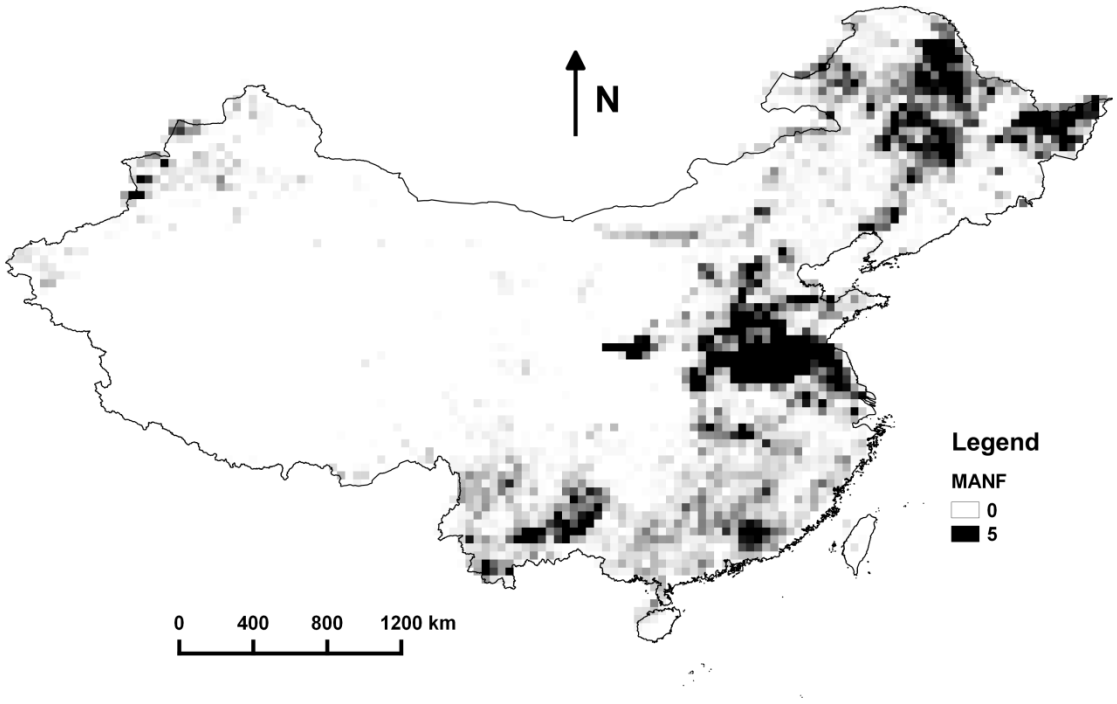

b)

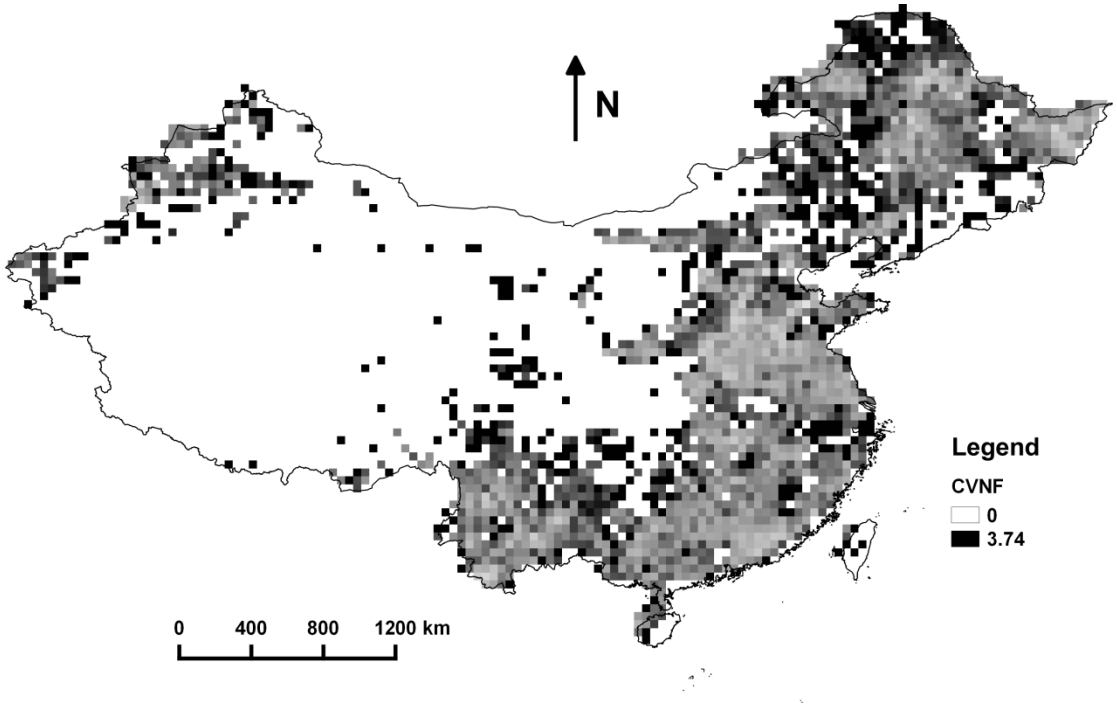

Figure 3 Maps of fire frequency (a) and its inter-annual variability (b)

4.1.2 Area burned and its inter-annual variability

The spatial distribution of MAAB in China is positively correlated with the fire frequency. High mean annual burned area happened in the regions where wild fires occurred more often, as most fire-prone areas stated in 4.1.1. The rest part of China is less prone to fires, or fire free, caused by less annual number of fires, or no fires (Figure 4 a).

Similarly, the inter-annual coefficient of variation in annual area burned shares a similar distribution pattern with the inter-annual coefficient of variation in annual number of fires, which indicates areas with higher annual area burned are with less inter-annual variation, and vice versa (Figure 4 b).

4.1.3 Inequality in fire frequency and fire size

In Figure 5, highest Gini index in Northeast China, intensively in Xiao Xing'an Mountains (Heilongjiang) and dispersedly in Great Xing'an Mountains (Inner Mongolia), and few areas in East and most west of China, shows that in those areas larger fires happened in less number of fires. Relatively lower Gini index in most part of southern China indicates that smaller fire size occurred in higher number of fires. Zero Gini index indicates that in some areas where only one fire appeared during the 14 years, and some other areas where fire size is equal in a very few number of fires (<=3).

4.1.4 Fire intensity

Fire radiative power retrieved from active fire data presents a map of larger fire affected areas in China (Figure 6). Extremely high fire radiative power is detected mostly in Northeast China in Great Xing'an Mountains and Xiao Xing'an Mountains (Inner Mongolia and Heilongjiang) covered with forests, and Southwest China in Hengduan Mountains (Sichuan and Xizang) covered with grasslands. Higher fire radiative power in Southeast China other than the rest of China land is also found. Those lands are covered with forests and savannas. In contrast, low fire radiative power exists in lowlands in eastern and part of central China, where cropland is the predominant land cover type.

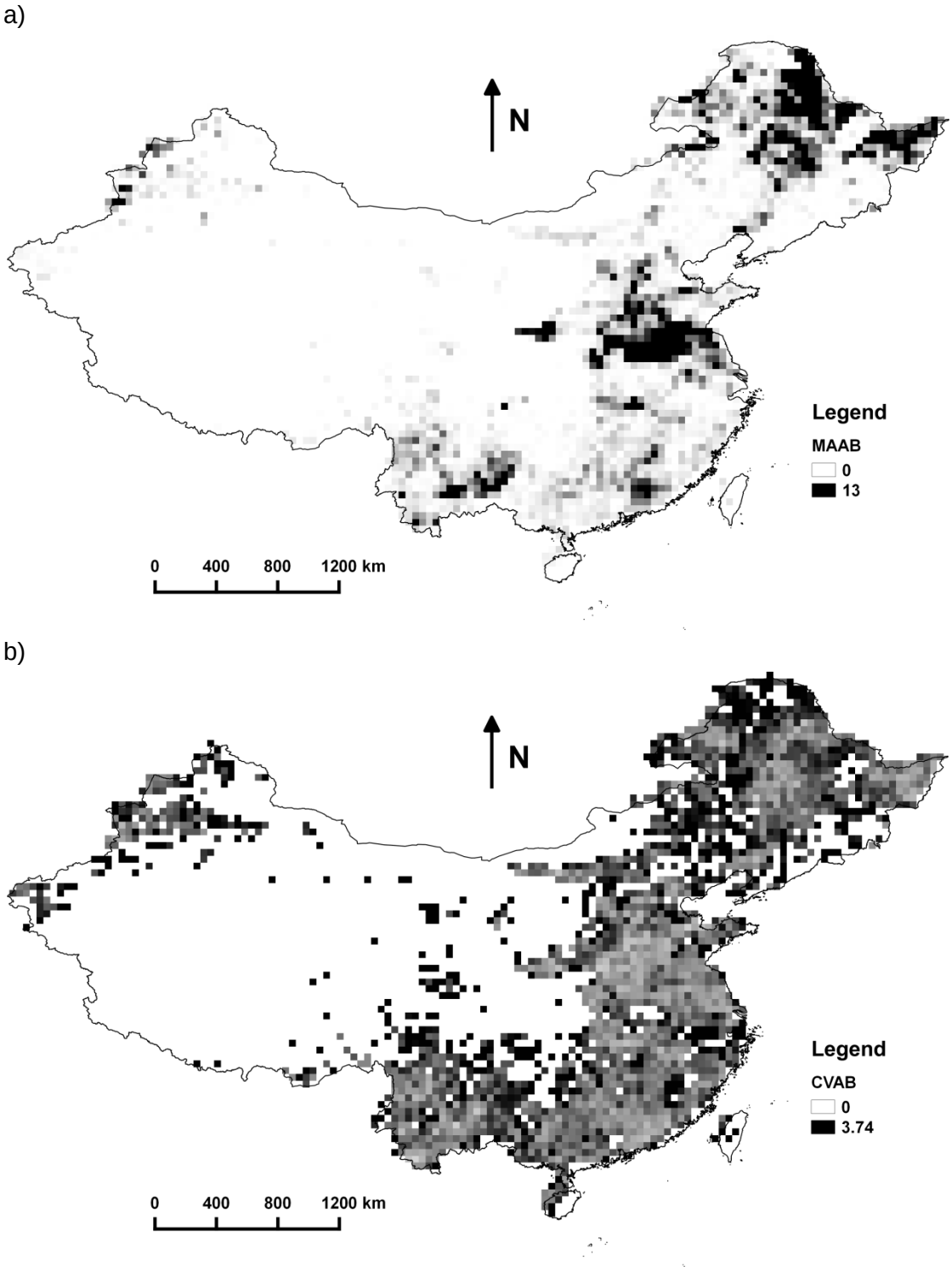

Figure 4 Maps of annual burned area (a) and its inter-annual variability (b)

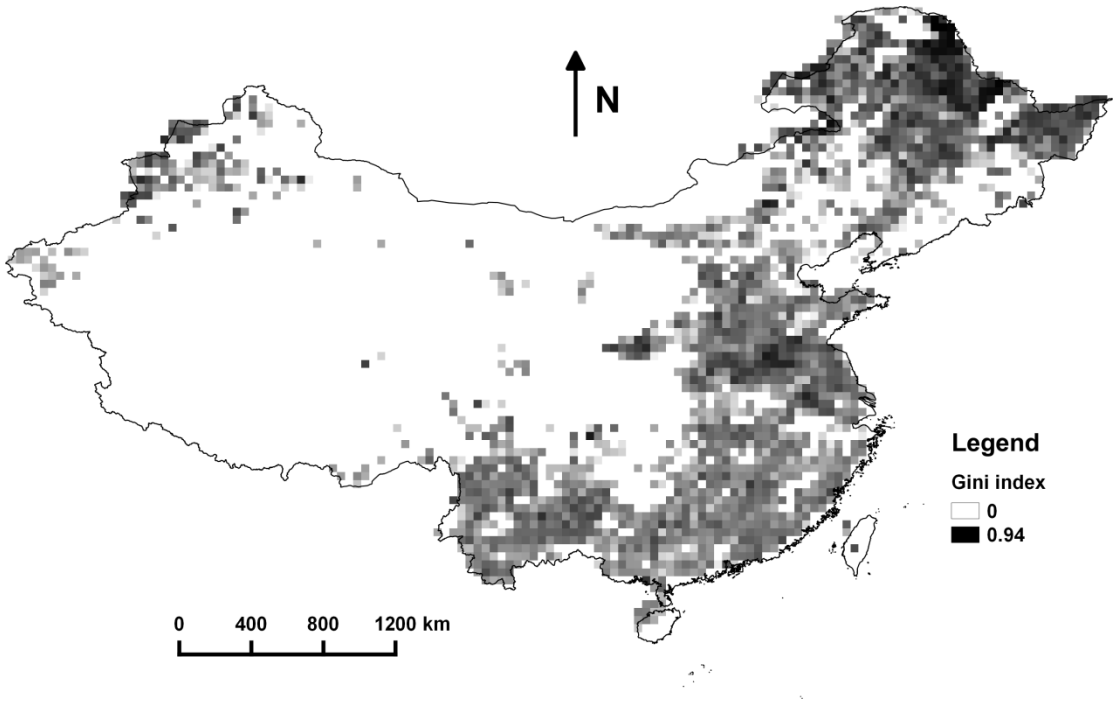

Figure 5 Map of fire frequency-size inequality from Gini index

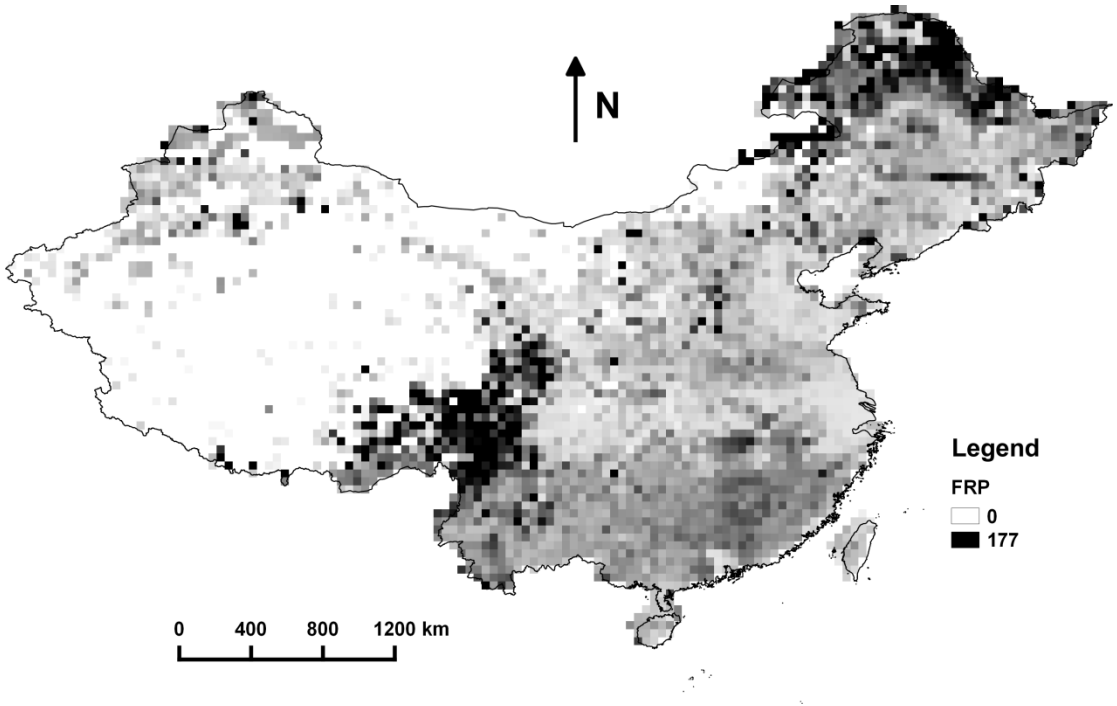

Figure 6 Map of fire intensity from the 90th percentile of fire radiative power

4.1.5 Fire seasonality

In Figure 7 a, the fire season duration is very long in South China especially in the boundary of four provinces (Guangdong, Hunan, Jiangxi, and Fujian), which lasts more than 9 months, followed by the fire season duration in Northeast China in Heilongjiang, which lasts more than half of a year. The fire season in Southwest China is with less than 3 months, while in part of East and Northeast China, and central and western China the fire season is shorter than one month.

The peak month occurred primarily in winter season in southern China, in spring and autumn season in northeastern and western China and in summer and autumn season in eastern China (Figure 7 b). The peak season is generally not in winter in northern areas and not in summer in southern areas. Much more fire pixels in peak month accumulated in the areas where are with higher fire frequency and larger burned area in all 14 years, and vice versa (Figure 7 c).

4.1.6 Land cover types affected by fires

The percentage of land cover types affected by wild fires is determined by the land cover of China. Forest and savanna areas are mostly affected by fires in southern and northeastern China and partly in eastern China (Figure 8 a, b). Grasslands are affected by fires mainly in Great Xing'an Mountains and Xiao Xing'an Mountains in northeastern China, Hengduan Mountains in southwestern China and Tianshan in western China (Figure 8 c). Croplands are affected by fires primarily in lowlands in East and Northeast China, and few areas in western China (Figure 8 d).

a)

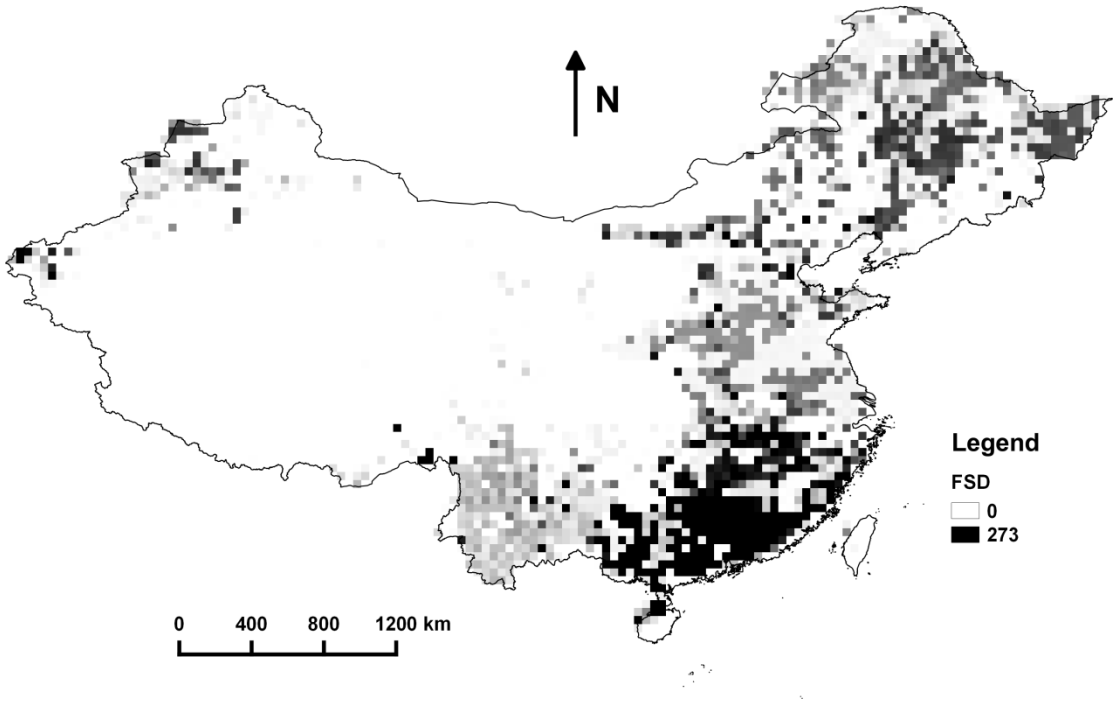
N
Legend
FSD
0
273
0 400 800 1200 km

b)

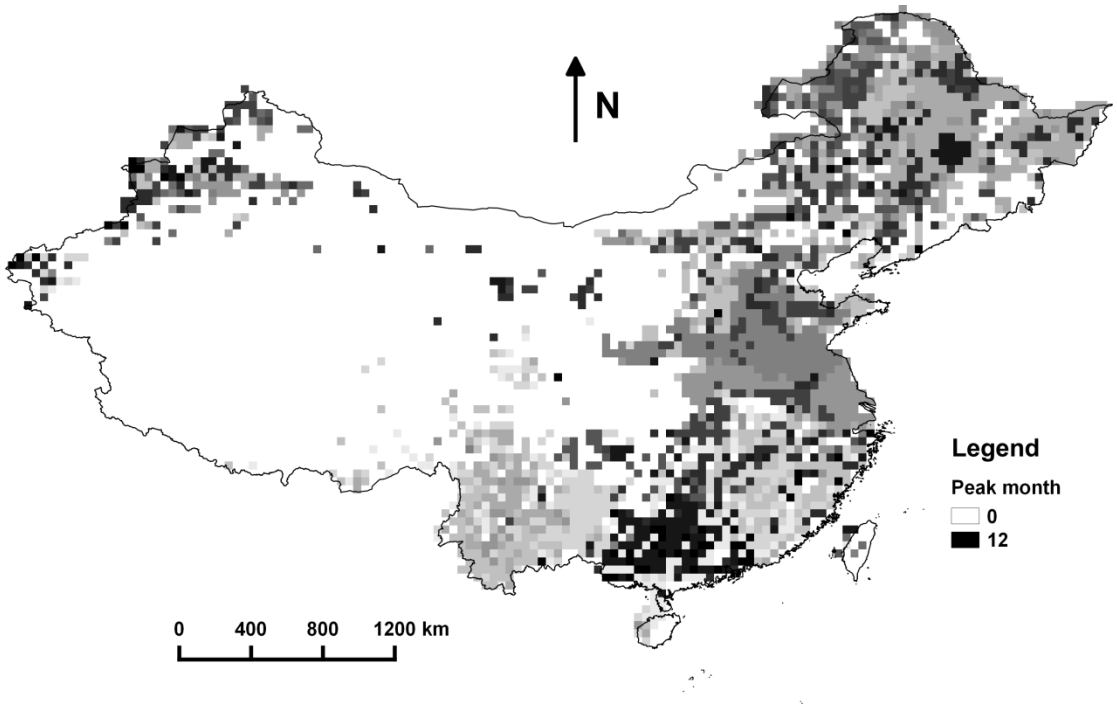
N
Legend
Peak month
0
12
0 400 800 1200 km

c)

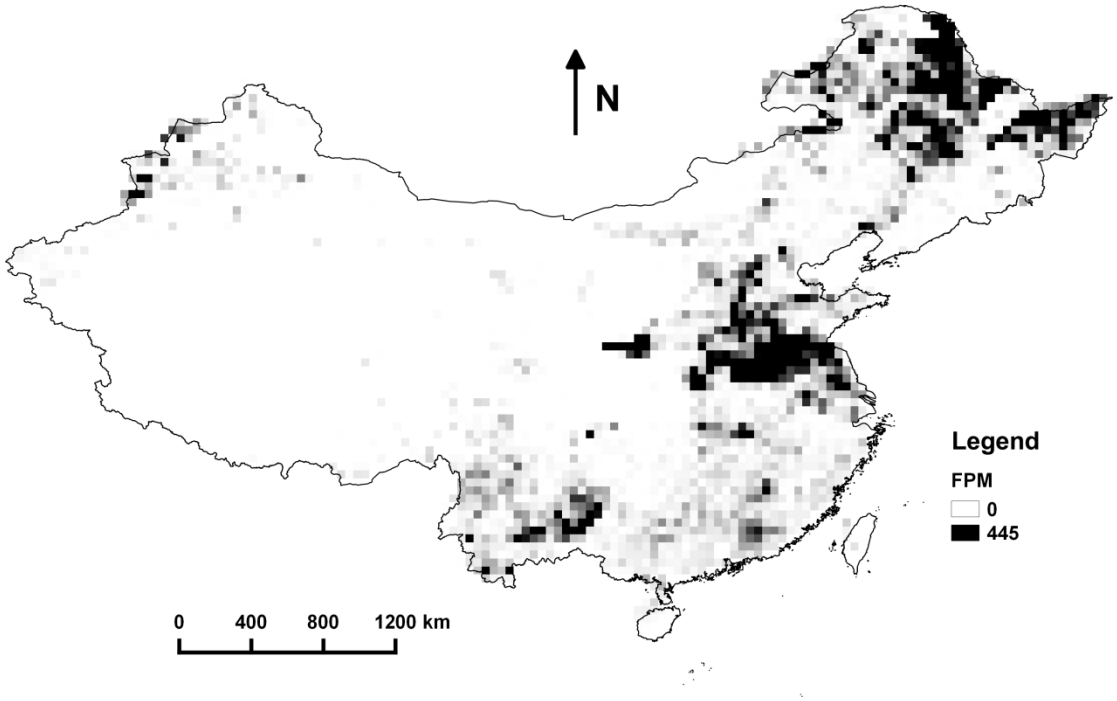

Figure 7 Maps of fire seasonality from fire season duration (a), peak month (b) and its burned pixels (c)

a)

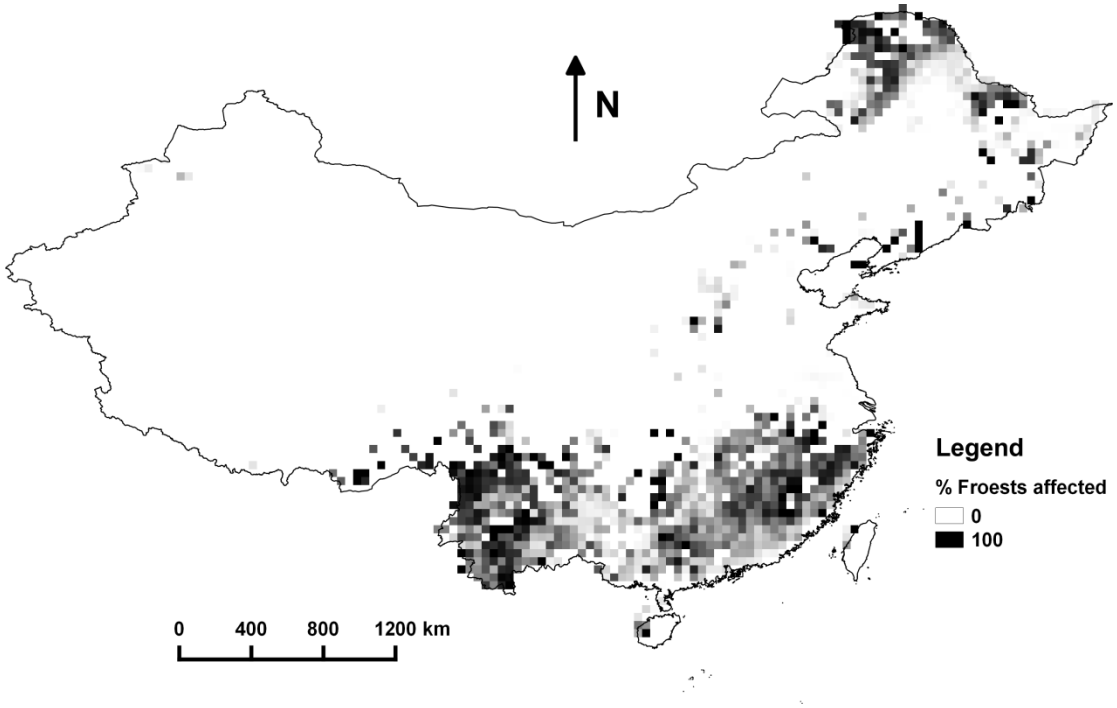
N
Legend
% Froests affected
0
100
0 400 800 1200 km

b)

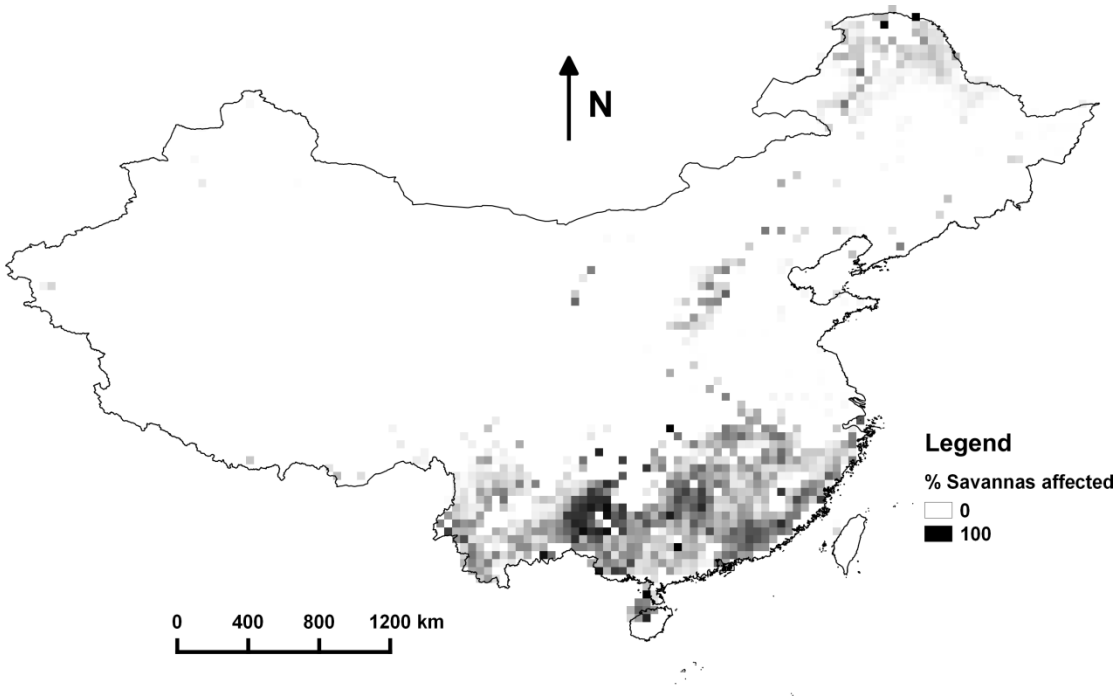
N
Legend
% Savannas affected
0
100
0 400 800 1200 km

c)

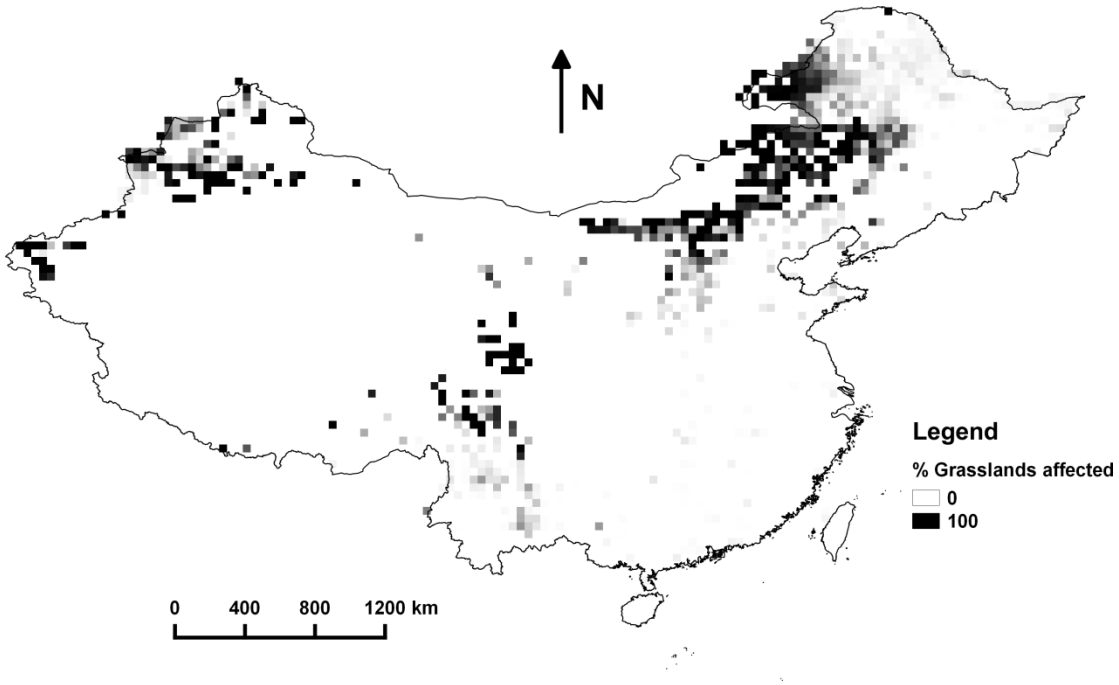

d)

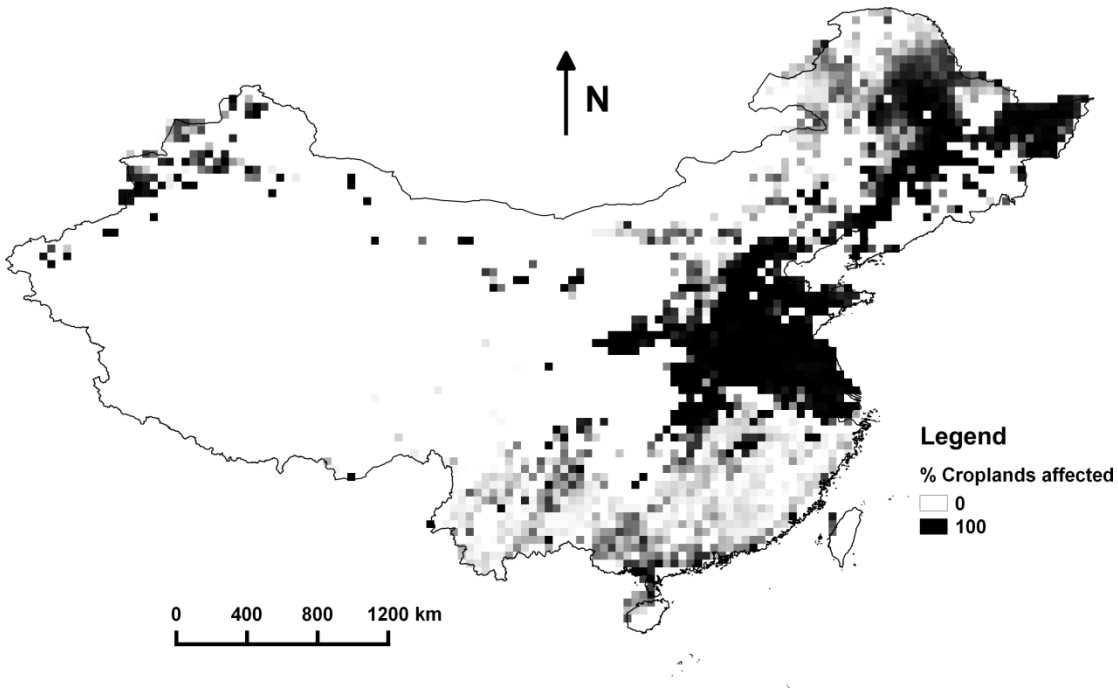

Figure 8 Maps of land cover types affected by fires from percentage of forests (a), savannas (b), grasslands (c), and croplands (d) affected

4.2 Factor analysis of fire regime variables

Figure 9 shows the data distribution of fire regime variables. The range of four variables, i.e. mean annual number of fires, mean annual area burned, fire radiative power, and fire pixels in peak month, is extremely high in very few numbers, indicating in a few regions the fire frequency, burned area and fire intensity are much higher than most areas in China. Most of the variables data are not normally distributed.

Table 1 shows the KMO and Fligner-Killeen test results. The KMO value indicates that the fire regime variables data are suitable for the application of factor analysis. Because the result of the Fligner-Killeen test of homogeneity of variances is significant, the hypothesis that all of the variances are equal can be rejected.

Table 1 Measures of suitability of data for factor analysis: Kaiser-Meyer-Olkin (KMO) and Fligner-Killeen test

KMO	Fligner-Killeen test		
	χ^2	d.f.	*p*
0.697	5278.6	11	<0.0001

The principal component analysis explained 82.51% of the original variance using the first five components and those five components were retained as they cumulatively explain at least 80% of variation (Table 2).

The communality for a given variable can be interpreted as the proportion of variation in that variable explained by the five factors. The communalities or proportion of variability extracted from most of the fire regime variables with principal component analyses are very high, except fire radiative power and percentage savannas affected by fires both show a relatively lower value below 70% (Figure 10). This result means that the variables are well explained by the components.

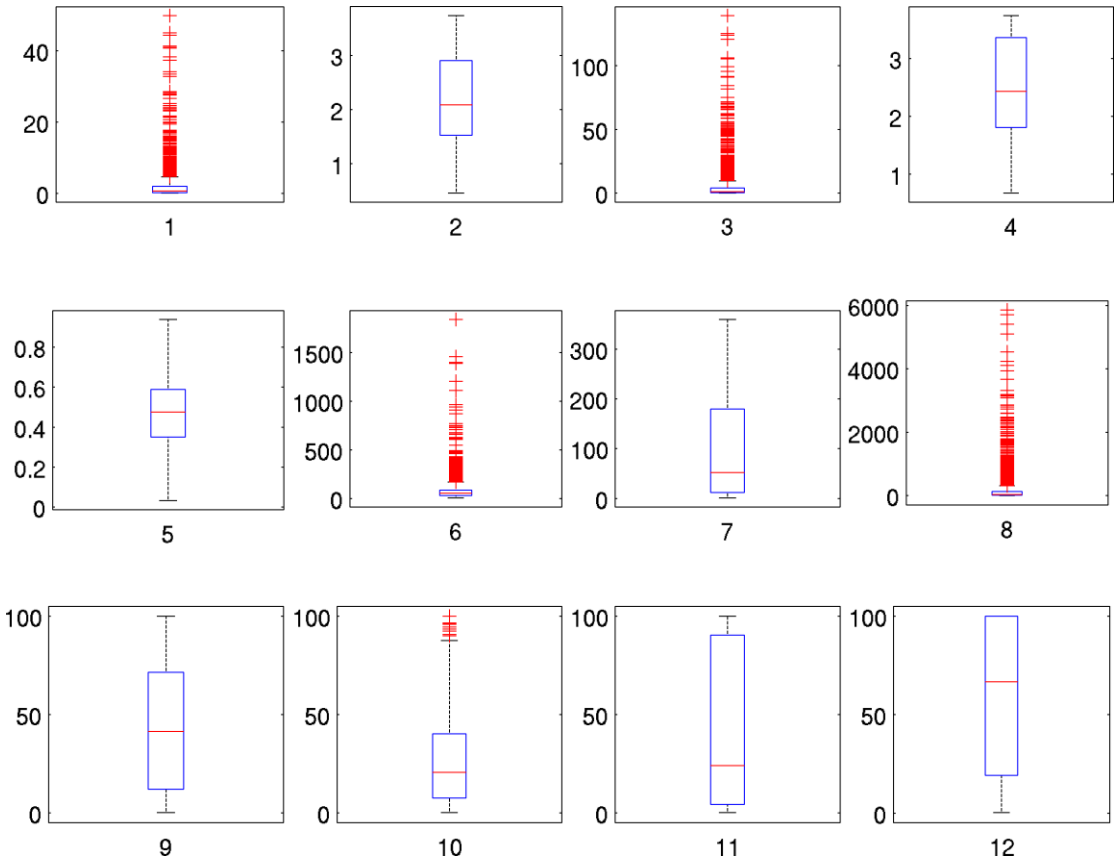

Figure 9 The box-plot distribution in values of fire regime variables

1: Mean annual number of fires; 2: Inter-annual coefficient of variance in annual number of fires; 3: Mean annual area burned; 4: Inter-annual coefficient of variance in annual area burned; 5: Gini index of fire sizes; 6: 90th percentile of fire radiative power; 7: Fire season duration; 8: Fire pixels in peak month; 9: Percentage forests affected by fires; 10: Percentage savannas affected by fires; 11: Percentage grasslands affected by fires; 12: Percentage croplands affected by fires.

Table 2 Results of the principal component analysis

Components	Eigenvalues		
	Total	Percentage of variance	Cumulative %
1	93.367	31.194	31.194
2	61.553	20.565	51.758
3	37.520	12.535	64.294
4	30.926	10.332	74.626
5	23.588	7.881	82.507
6	19.729	6.591	89.098
7	15.078	5.037	94.135
8	8.369	2.796	96.932
9	5.073	1.695	98.626
10	2.899	0.968	99.595
11	0.872	0.291	99.886
12	0.342	0.114	100.000

The correlation among fire regime variables and the chosen components are shown in Table 3. The higher absolute values in the table indicate stronger correlation between the variables and the principal components. PC 1 and PC 2 are both more strongly correlated with the fire regime variables associated with burned area and number of fires, but PC 1 has a higher correlation with the distribution of fire size in number of fires and annual burned area, whereas PC 2 is more correlated with the inter-annual variability of burned area and number of fires. There are different higher correlations among principal components and land cover related variables (PC 3 with savanna, grassland and forest, PC 4 with cropland and forest, and PC 5 with grassland and forest). PC 3 and PC 5 are both more correlated with fire season duration but in the opposite directions (-0.39 and 0.54). PC 4 is also more strongly corrected with fire intensity (0.62). However, those correlations are not very strong to determine the principal components with single fire regime variables.

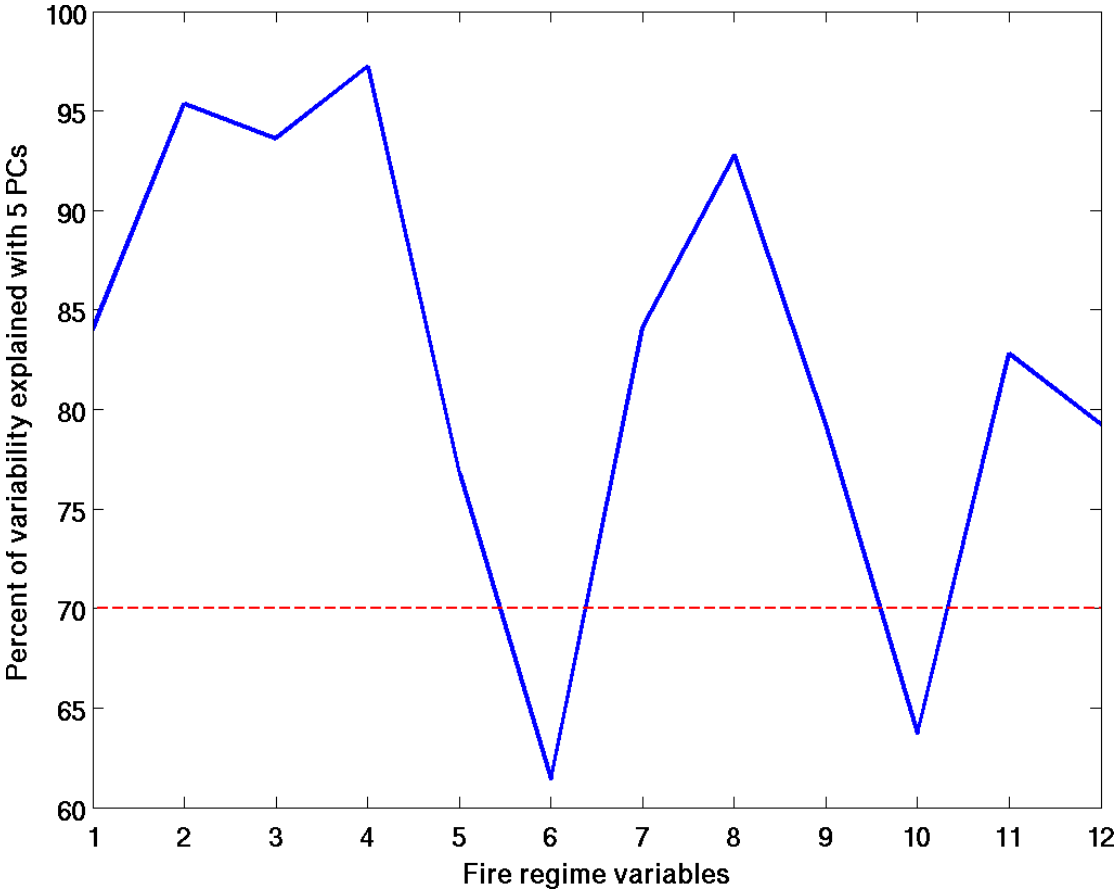

Figure 10 Percentage of variability explained by fire regime variables

1: Mean annual number of fires; 2: Inter-annual coefficient of variance in annual number of fires; 3: Mean annual area burned; 4: Inter-annual coefficient of variance in annual area burned; 5: Gini index of fire sizes; 6: 90^{th} percentile of fire radiative power; 7: Fire season duration; 8: Fire pixels in peak month; 9: Percentage forests affected by fires; 10: Percentage savannas affected by fires; 11: Percentage grasslands affected by fires; 12: Percentage croplands affected by fires.

Table 3 Correlation among fire regime variables and principal components

Fire regime variables	PC 1	PC 2	PC 3	PC 4	PC 5
1. MANF	-0.38	0.34	-0.01	0.03	-0.02
2. CVNF	-0.27	-0.45	0.27	-0.06	-0.27
3. MAAB	-0.40	0.33	0.00	0.20	-0.05
4. CVAB	-0.30	-0.44	0.25	-0.06	-0.24
5. Gini index	-0.43	-0.08	-0.10	-0.08	0.20
6. FRP	-0.10	-0.11	0.05	0.62	0.26
7. FSD	-0.21	-0.20	-0.39	-0.25	0.54
8. FPM	-0.39	0.34	0.03	0.21	-0.10
9. % forests affected	-0.13	-0.31	-0.37	0.31	-0.42
10. % savannas affected	-0.13	-0.24	-0.52	0.03	0.13
11. % grasslands affected	-0.05	-0.22	0.51	0.19	0.52
12. % croplands affected	-0.31	0.09	0.14	-0.56	-0.02

4.3 Fire regime classification

According to the elbow method, the scree plot in Figure 11 shows that the most appropriate number of clusters should range between 2 and 4. The results obtained in our simulations show that two or three clusters are not enough to differentiate fire regimes in China before 4 as the number of clusters was chosen. Therefore, four fire regimes are revealed in China.

The spatial distribution of fire regimes M, R, B, and G in China are showed in color magenta, red, blue and green in Figure 12. The comparisons among fire regimes and variables are shown in Table 4, where fire pattern is described in area burned and land cover. Figure 13 shows the four cluster centroids resulting from k-means analysis based on the five principal components. These clusters differ significantly according to a MANOVA.

Fire regime M covers the most of central China (Inner Mongolia, Ningxia and Xizang, and Gansu, Qinghai, Shannxi, Sichuan, Chongqing, Hubei, and Guizhou), and extends to western (Xijiang), northeastern (mainly in Jilin), southern China (Hainan and Taiwan islands), where no fires detected by burned area data, which is

around 36.5% of fire affected area in China. Since the fire characteristics except fire intensity are defined by burned area data, in those regions with fire regime M there is not a clear fire pattern showed in any of the fire regime descriptors. The fire intensity is low in central China and most of other regions in cluster M, but exhibits very high values in Hengduan Mountains regions (Figure 6).

Fire regime R represents most fire prone areas, exists mainly in the boundary area among Shandong, Jiangsu, Henan and Anhui in East China and the boundary area between Inner Mongolia and Heilongjiang in Northeast China. It is the smallest category and includes, only around 3.3% of the fire grid cells. Very few areas cover with fire regime R sparsely in Northeast, East, Southwest and West China. Those areas are clustered because of high MAAB and FPM.

The rest of China shows low MAAB and FPM based on burned area data and is divided into two regimes by land cover types. Fire regime B, taking up about 38.1% of fire affected area, exists predominantly in cropland and grassland in Northeast (Inner Mongolia, Heilongjiang, Jilin, and Liaoning), North (Hebei, Shanxi, Shandong, Henan), East (Jiangsu, Anhui, Zhejiang, and Jiangxi), central (a larger area in Hubei and fragmented areas in other regions) and West (Xinjiang) China. Fire regime G is found in northern (Inner Mongolia and Heilongjiang) and southern China (Yunan, Guizhou, Hunan, Jiangxi, Zhejiang, Fujian, Guangdong and Guangxi) mainly covered with forest and savannas, and includes approximately 22.1% of the fire grid cells.

Figure 14 concludes the classification of fire regimes in China. Fire regime M differs from the other three fire regimes dues to the using of fire radiative power from active fire data as a fire regime variable. Mean annual area burned is the main fire characteristic differentiates fire regime R from the rest of two fire regimes. However, comparing other fire characteristics including inter-annual variability, intensity and seasonality listed in Table 4, it is difficult to show distinct patterns in each fire regime.

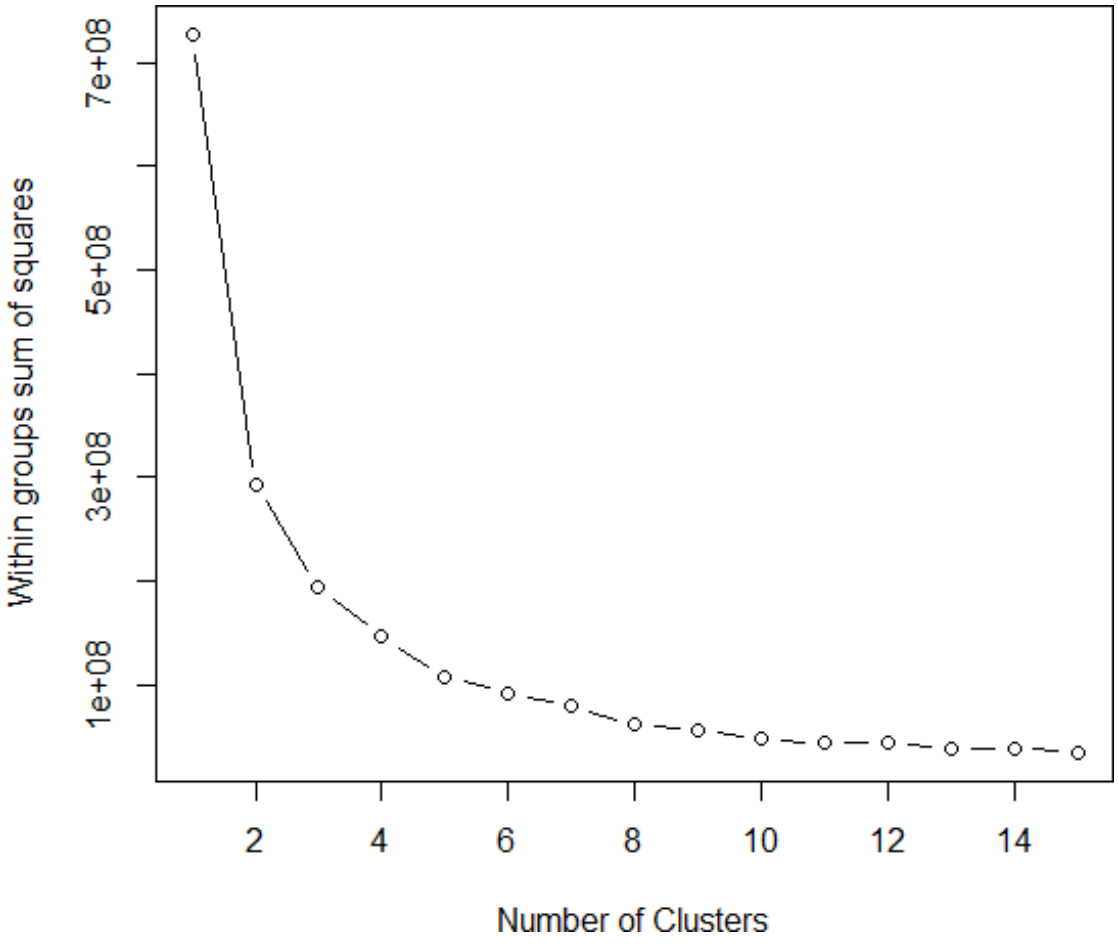

Figure 11 Scree plot of within groups sum of squares by number of clusters

a)

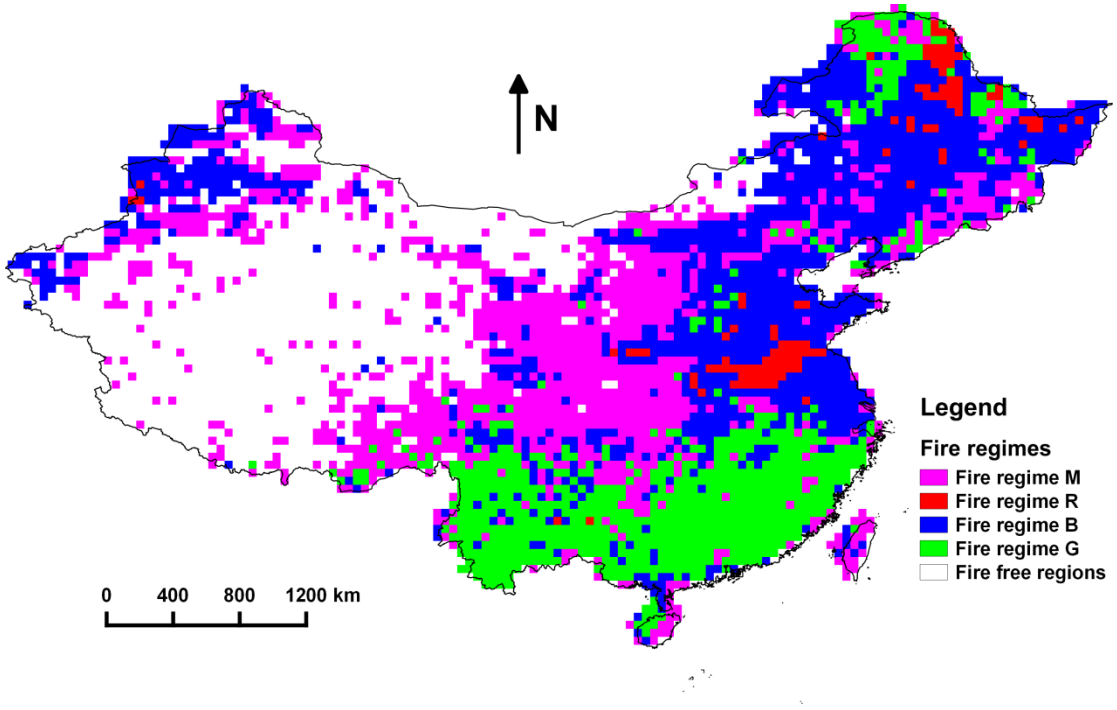
N
Legend
Fire regimes
Fire regime M
Fire regime R
Fire regime B
Fire regime G
Fire free regions
0 400 800 1200 km

b)

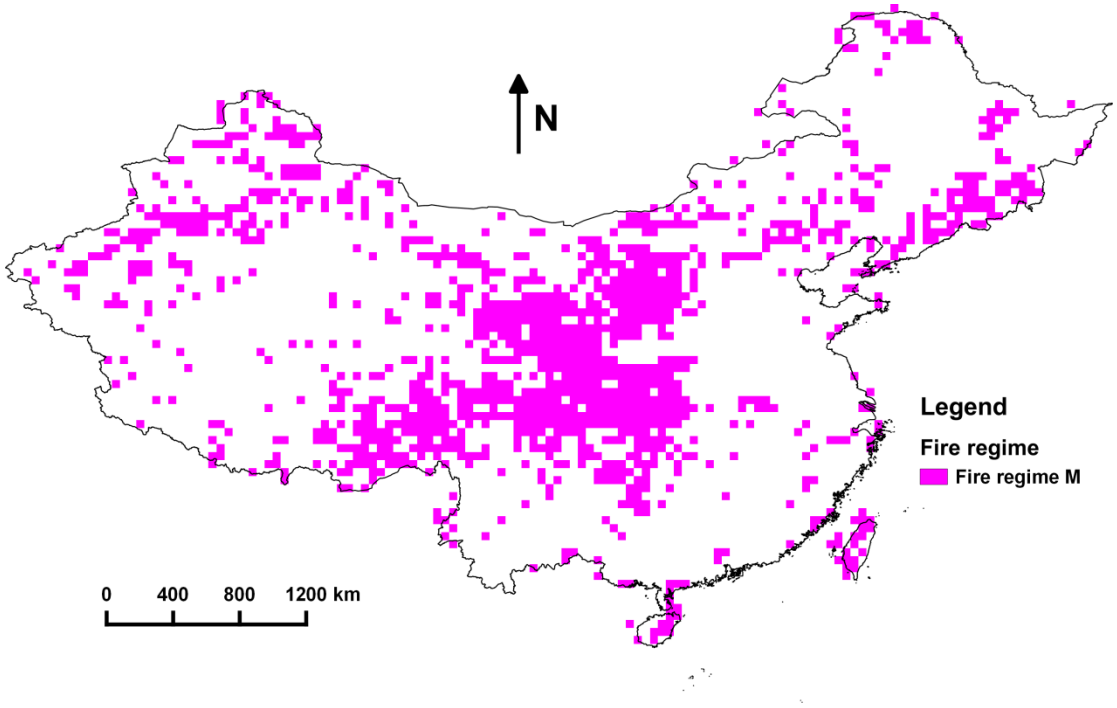
N
Legend
Fire regime
Fire regime M
0 400 800 1200 km

c)

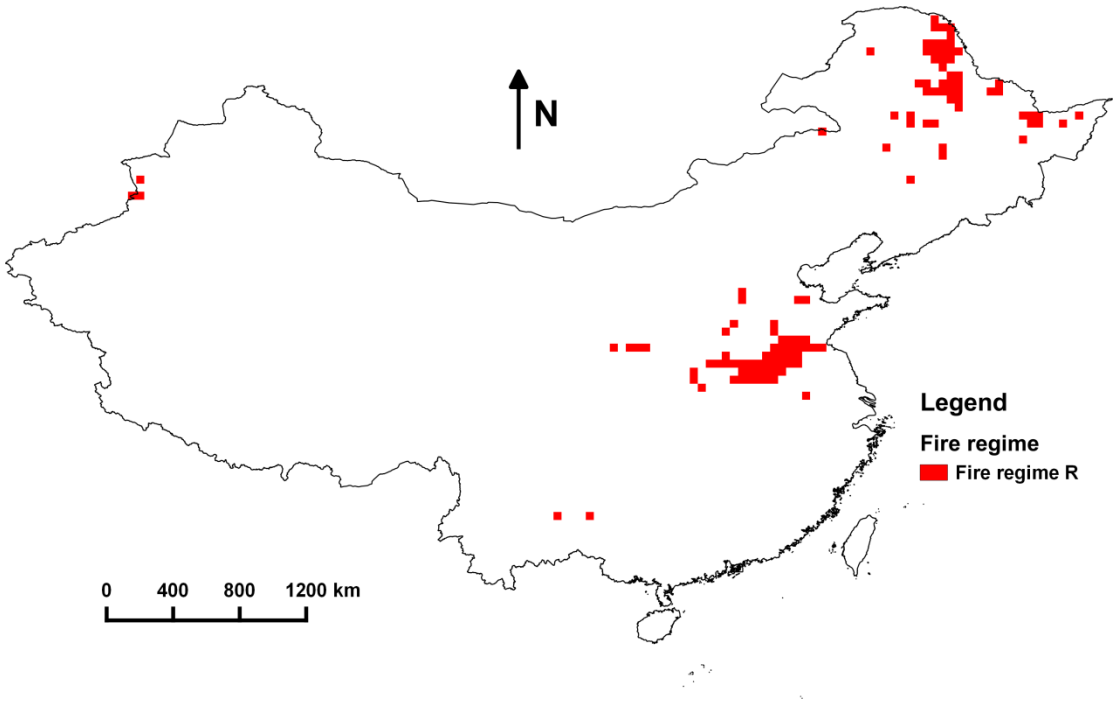
N
Legend
Fire regime
Fire regime R
0 400 800 1200 km

d)

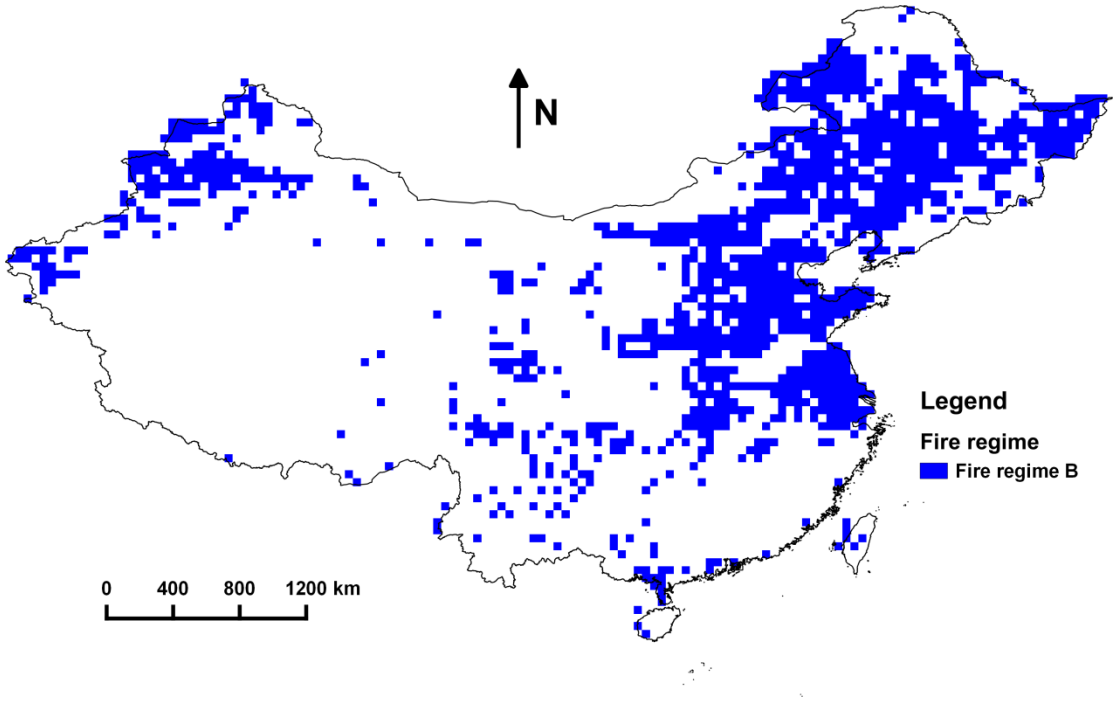
N
Legend
Fire regime
Fire regime B
0 400 800 1200 km

e)

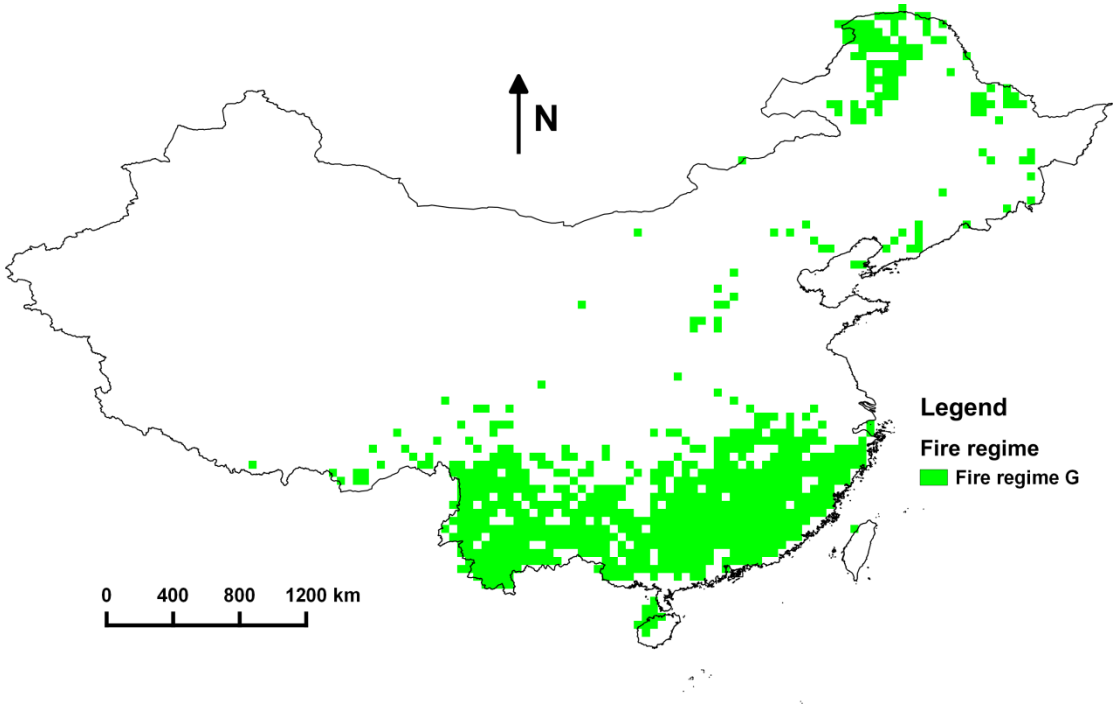

Figure 12 Maps of fire regimes (a), fire regime M (b), fire regime R (c), fire regime B (d), and fire regime G (e)

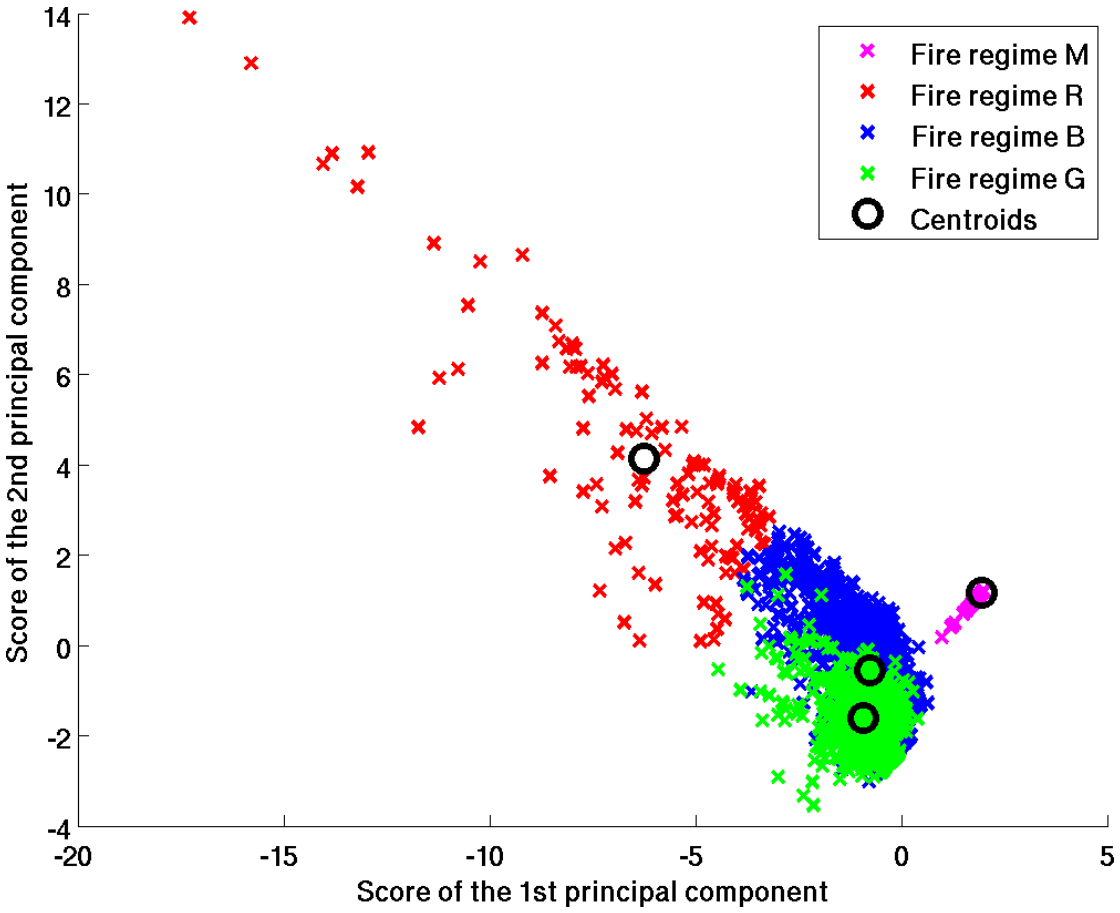

Figure 13 Cluster centroids of fire regimes measured by five principal components

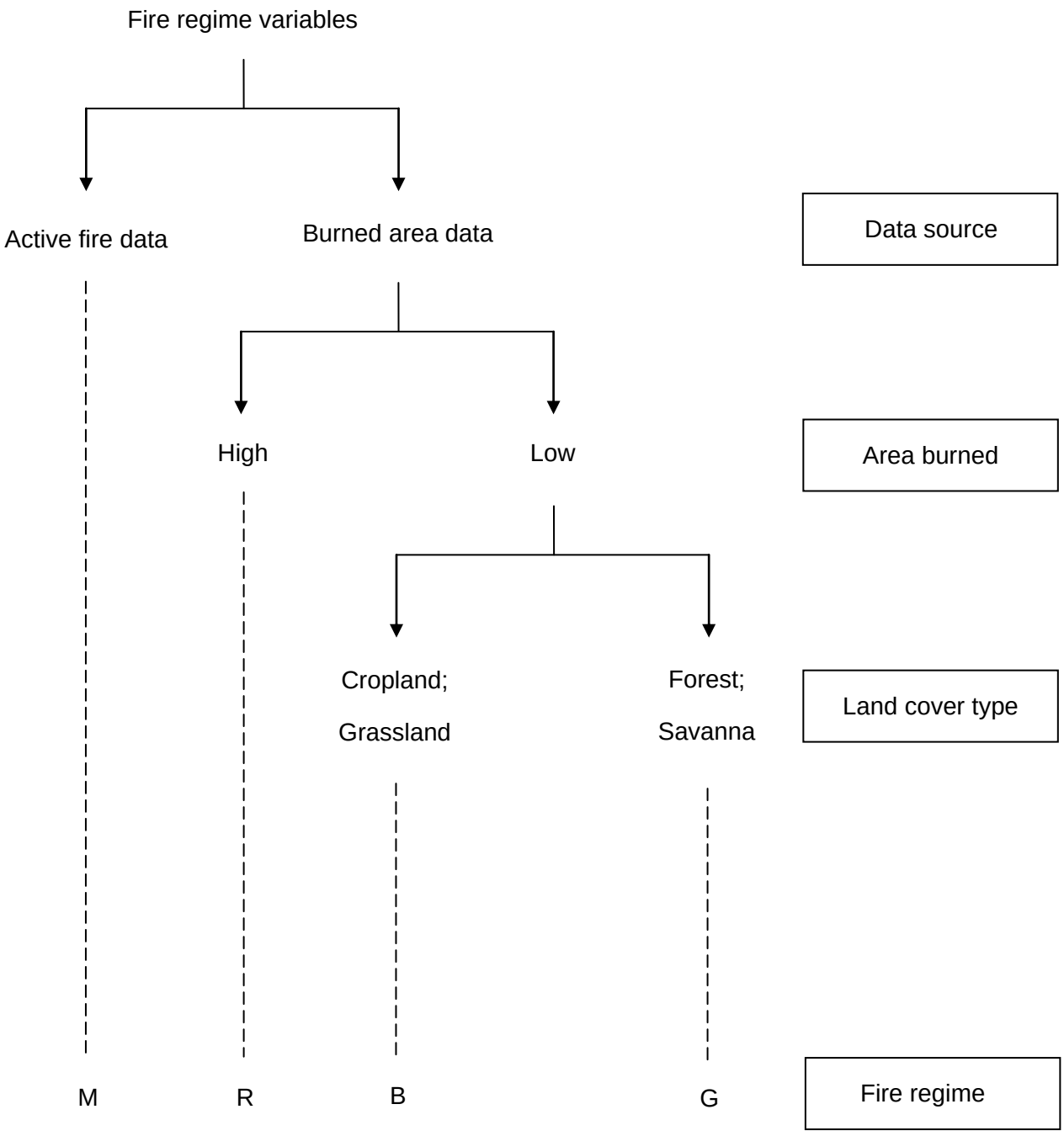

Figure 14 Classification of fire regimes

Table 4 Comparisons among five regimes in China

Fire regimes		M	R	B	G
Fire pattern		Unknown	HCF	LCG	LFS
Number of cells		1274	117	1330	772
Main location		Central	Northeast; East	Northeast; East; West	South; North
Comparisons in predominant fire characteristics	Frequency	NA	High	Low	Low
	Burned area	NA	High	Low	Low
	Variability	NA	High/Low	High/Low	High/Low
	Intensity	High/Low	High/Low	Low	High
	Fire season	NA	Short	Long/Short	Long/Short
	Land cover affected	NA	Cropland; Forest	Cropland; Grassland	Forest; Savanna

HCF: High annual and peak month area burned, Cropland and Forest; LCG: Low annual and peak month area burned, Cropland and Grassland; LFS: Low annual and peak month area burned, Forest and Savanna.

5. Discussion

5.1 Remote sensing of fires

Vegetation burning is a global scale environmental phenomenon, in which the large extent of fire-affected areas and the low accessibility of many key fire regions make remote sensing an indispensable fire research and monitoring tool. Various space and airborne sensors have been applied in assessing characteristics of active fires and post-fire ecological effects, and numerous remote sensing tools and techniques have been employed to quantify and monitor fire-related processes that cause change in soil and vegetation (Lentile *et al.*, 2006). The utility of satellite data for mapping fire-affected areas and characterizing the properties of wildfires is an area of active research, nevertheless, the accuracy and consistency of those products have not been definitively demonstrated and the results of global fire characteristics concluded from remotely sensed data have not been validated widely (Roy *et al.*, 2013).

MODIS active fire and burned area products were both applied in the computation of fire regime variables in this study. However, their correlation during the study period in either counts of detections (Figure 15 a) or days of detections (Figure 15 b) is very low. Although the fluctuations of active fire counts and burned pixels during the 14 years show a similar pattern, higher frequency of active fire counts were detected obviously during most of the days of year (Figure 16). This can be explained by their differences in the fire detection algorithms and the spatial resolutions (Table 5). The combined use of such two datasets has assisted in the identification of fire regimes in China.

a)

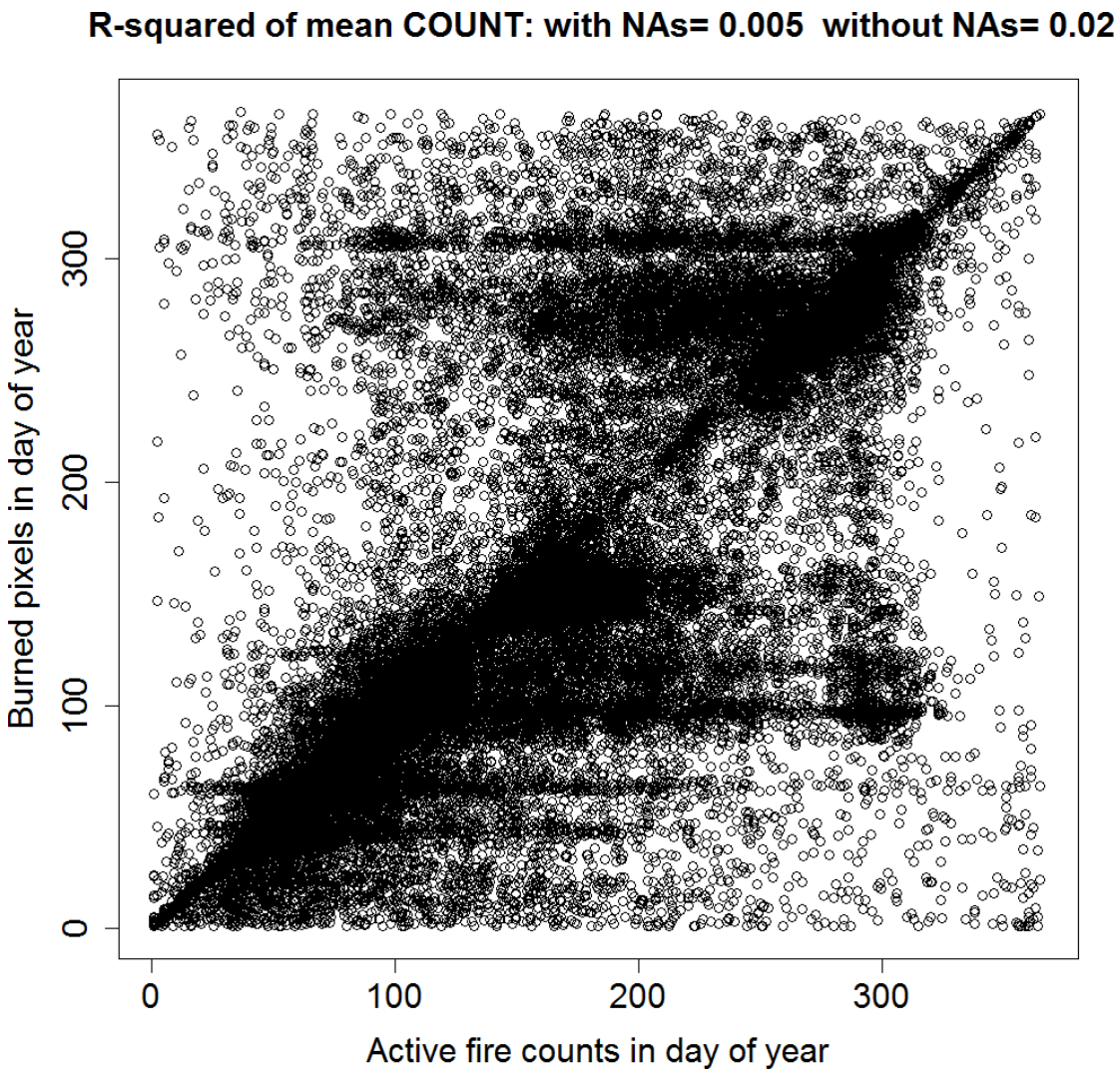
R-squared of mean COUNT: with NAs= 0.005 without NAs= 0.02
Burned pixels in day of year
0
100
200
300
0
100
200
300
Active fire counts in day of year

b)

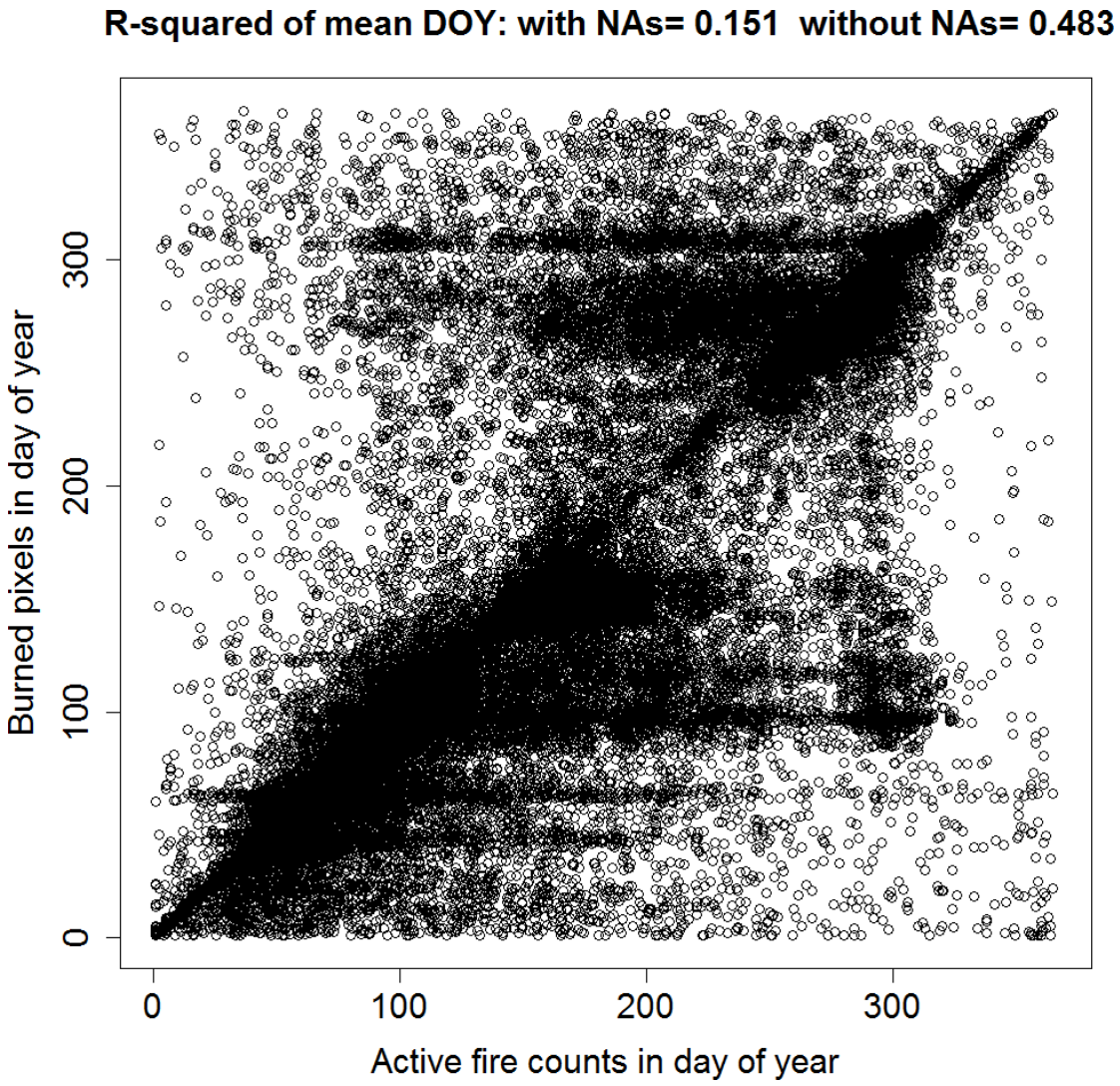

Figure 15 Correlation in the count of points (a) and the mean of day of year values (b) within the same geo-grid between active fire counts and burned area pixels (2001-2014, China)

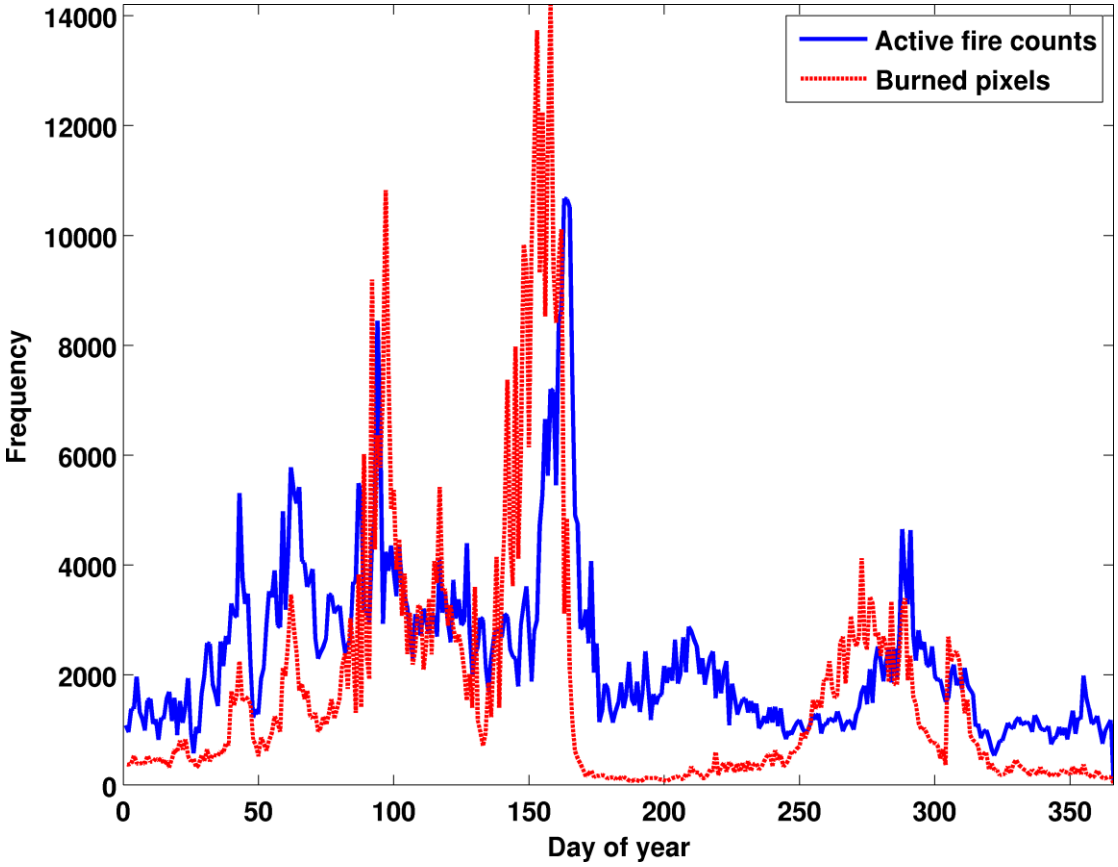

Figure 16 Frequency of active fire counts and burned pixels in day of year (2001-2014, China)

Table 5 Comparisons between active fire data and burned area data used

	Active fire data	Burned area data
MODIS products	MCD14ML	MCD64A1
Spatial resolution (km)	1.0	0.5
Detection basis	Temperature	Surface reflectance
Spectral bands (μm)	4.0, 11.0, 12.0	0.65, 1.2, 2.1
Minimum detectable size (ha)	~ 0.12	~ 120
Limitation	Large fires	Small fires
Reference	Giglio *et al.* 2003	Giglio *et al.* 2009

Active burning fires can be differentiated by detecting the elevated energy released relative to their non-burning surroundings at middle-infrared to thermal wavelengths (i.e. 3.6 - 12μm), which depends on the temperature even when the fire covers small fractions of the pixel (Lentile *et al.*, 2006; Roy *et al.*, 2013). Unfortunately, some issues are related to the use of this fire detection algorithm, specifically, it is affected by the following limitations. Only pixels containing active fires at the time of satellite overpass are identified. Fires that move quickly across the landscape relative to the satellite observation frequency will not be detected. The detection of active fires can also be missed due to the obstacles such as cloud or thick smoke obscuration and overstory vegetation. Certain fires may be too small or cool to be detected.

Comparatively, post-fire burned area is detected from a drastic reduction in visible-to-near-infrared surface reflectance (i.e. 0.4 - 1.3μm) associated with the charring and removal of vegetation, accompanied by a rise in short wave infrared reflectance (i.e. 1.6 - 2.5μm) and brightness temperatures, which is attributed to the combined effects of increased soil exposure, increased radiation absorption by charred vegetation, and decreased evapotranspiration relative to the pre-fire green vegetation (Lentile *et al.*, 2006). But some limitations of this fire detection algorithm should be considered. Tree canopy or cloud cover can obscure the post-burn, top-of atmosphere radiometric signal of burns from surface fires. The algorithm can confuse recently cleared, unburned forest patches with burned areas in case of tropics undergoing deforestation, especially when the deforestation slash is piled within the clearing and subsequently burned after a short drying period (Giglio *et al.*, 2009).

Based on above fire detection algorithms, both active fire and burned area data have their advantages and disadvantages. Comparing with the minimum detectable size of a burned area, which is very much larger than the typical size of agriculture waste and deforestation burns, the minimum detectable size of an active fire can be 1000 times smaller (Giglio *et al.*, 2009). However, with active fire detections from polar-orbiting satellites it is difficult to capture large fires: indeed, they typically underestimate the temporal dynamics of fire, and the spatial extent of fire-affected areas where the fire progresses rapidly across the landscape (Roy *et al.*, 2013).

Burned area products are more reliable in detecting medium and large fires. In this study, active fire algorithm detected ~67% of land affected by wildfires in China, which is ~24% more than the fire-affected area detected by burned area algorithm. These exclusive grid cells in burned area data are identified in fire regime M, highlighting central China, where probably those types of fires occurred: small and less frequent fires; or surface fires in forests; or burned area recovered quickly in grasslands and croplands. These areas were excluded in previous global studies because they only considered the areas overlapped by the availability of remotely sensed datasets (Archibald *et al.*, 2013) or discarded the active fire data below their threshold (Chuvieco *et al.*, 2008).

5.2 Characteristics of fires and their potential drivers

The control of fires at different temporal spatial scales is driven by different environmental factors, and climate, landscape and vegetation are the dominant drivers of regional fire regime in decades. Moreover, recently the discussion on the role of anthropogenic factors (e.g. population density, land-use practices, livestock grazing, and road density) in fire regime has increased significantly (Archibald *et al.*, 2009; Le Page *et al.*, 2010; Lehsten *et al.*, 2010; Pausas & Fernández-Muñoz, 2012; Zumbrunnen *et al.*, 2012; Knorr *et al.*, 2014). Forest fires and agricultural burning are mostly caused by human activities in China. The characteristics of fires such as annual area burned and seasonality are expected to be greatly influenced by human activities through fire ignition, fire spread and fire extinction, which also indirectly impact fire size and intensity, comprehensively or selectively coupling with the impact of dominant drivers in different regions in China.

The HCF fire pattern in fire regime R indicates that significant fire activity occurred mostly in Northeastern and Eastern China in croplands, with a lower level of inter-annual variability. In these most fire-prone regions, it is expected that fire activity is caused by human activities. But the fire ignition source of a small fraction of high MAAB in Great Xing’an Mountains and Xiao Xing’an Mountains forest areas with

higher inter-annual variability in HCF pattern area is more likely to be triggered by lighting strokes in spring. The increasing forest fire danger in this region could have resulted from the increase in the maximum temperature and the decrease in precipitation and humidity (Niu & Zhai, 2012). The higher Gini index in this proportion of forest fires indicates that more large fires happened in this region where a certain environmental condition tends to support fire spread.

Fires occurred in LCG (fire regime B) and LFS (fire regime G) areas, where MAAB and FPM are both relatively lower and inter-annual variability in fire frequency and burned area highlights differently in different regions and vegetation types. The forest fires have mainly low inter-annual variation of fire activity in southern regions but mainly high inter-annual variation of fire activity in northern regions, indicating different causes of fires in these two regions. Cropland fires show relatively low inter-annual variability whereas grassland fires show relatively high inter-annual variability. These fire regimes are also supposed to largely link with climatic and anthropogenic factors. A positive correlation between burned area in forests and temperature was found in most regions in China (Lv, 2011). Liu *et al.* (2012) showed that the predicted change in overall fire occurrence density is positively related to the degree of temperature and precipitation change, but the spatial pattern of change is expected to vary spatially according to proximity to human ignition sources.

The seasonality of cropland fires is with peak month mostly in spring and autumn and longer fire season duration in Northeast China Plain and it is with peak month also in summer (concentrated in East China in June) and shorter fire season duration in North China Plain, probably due to different agricultural practices. The fire season duration of forest and savanna fires in LFS pattern shows a distinct regional pattern. It reveals a very short fire season in Northeast China, which normally ends within one month, and a longer fire season in most of Southwest China (less than 3 months), but a very long fire season in South China and part of Southeast China (more than 9 months). However, savanna fires in southern Guizhou (Southwest China) last less than one month with a peak in February. The peak month of forest and savanna fires mostly occurs in non-winter seasons in Northeast China, and non-summer seasons in

southern China. Similarly, the peak month of grassland fires in northern areas (Inner Mongolia and Xijiang) is not typically in winter and on the contrary winter is the peak season of grassland fires in Southwest China (Sichuan). Grassland fires are more likely last less than one month in western China.

The seasonality of vegetation fires in China is controlled by a combination of fuel condition, climate and human activities. Fire sensitivity in dry season varies in fine or dead vegetation (grasslands, savannas, croplands) which desiccate rapidly and prone to early season fires, and live and wooded vegetation (forests) which has slower moisture dynamic and likely to burn late in dry season (Le Page *et al.*, 2010). Climate variables play a very important role in fire season duration in China. Researchers in China have found that forest fires least likely happen when monthly average temperature below -10 °C or higher 15 °C and most likely happen if monthly average temperature between 0 to 10 °C, and when the monthly average precipitation reaches above 100 mm or annual precipitation is higher than 1500 mm and well distributed, forest fires are also unlikely to occur (Sun *et al.*, 2014). Therefore, the peak month of forest fires hardly occur in winter in northern China when the low temperature restrict fire occurrences and is not likely to occur in summer in southern China when the high precipitation reduces the burning probability. The long fire season duration in South China is expected to be mainly caused by human activities. It was found that temperature positively correlate with burned forest area, while precipitation negatively correlated with burned forest area in South China (Lv, 2011). However, forest fires in this region were largely ignited artificially from agricultural practices, because fire is a common agricultural tool in small scale family farms and most of the farms and plantations have a staggered distribution, agricultural and negligent uses of fire have become the major sources for forest fires (Tian *et al.*, 2013).

The frequency-size inequality of fires derived from Gini index in China displays a pattern of more large fires within less number of fires in north and more small fires within more number of fires in south, particularly in forests. Fuel, topography, weather, land use management and fire suppression efforts tend to have significant contribution to the inequality in fire size distributions through controlling fire behavior.

Vegetation flammability and continuality with characteristics of climate (e.g. strong winds and low humidity) and landscape (e.g. up slope and lower elevation) that favor fire spread can provide advantages for large fires. Removing fuel amount by thinning or using prescribed fires can prevent large fires if those large fires are a direct consequence of fuel accumulation, in which case, fire suppression efforts on small and frequent fires will lead to few larger fires.

A study on statistical models of the size distribution of lightning-caused wildfires in the boreal mixed wood forests in Canada showed that the expected size of a fire is positively related to the abundance of pine forest in the vicinity of the point of detection, and negatively related to the abundance of recently logged or burnt areas (Cumming, 2001). Another simulation modeling on the effect of fire-exclusion and prescribed fire on wildfire size in Mediterranean ecosystems provided some information that higher fire-fighting capacities resulted in a slightly higher proportion of large fires while the total amount and proportion of large fires decreased as the prescribed burning intensity increased (Piñol *et al.*, 2005). Moreover, Chang *et al.* (2007) simulated the long-term forest landscape responses to fire exclusion in the Great Xing'an Mountains by using their LANDIS model and showed that fire exclusion can lead to catastrophic fires with return intervals ranging from 50 to 120 years. These models could help explain the influence factors of large fires, such as large forest areas and intensive fire exclusion, in boreal mixed wood forests in Northeast China. The fires were ignited primarily by lightning, but forest harvesting and fire suppression have altered fire regimes from frequent and low intensity surface fires mixed with infrequent stand-replacing fires, with fire return interval ranged from 30 to 120 years, to infrequent but more intense, with a fire return interval of more than 500 years (Liu *et al.*, 2012).

On the contrary, more small and frequent fires occurred in southern mixed forests and evergreen woodlands. This happens to coincide with the finding that evergreen oak woodlands in Portugal exhibit a distinct pattern with fire avoidance increasing as fire size increasing (Barros & Pereira, 2014). Generally, large fires are not significantly selective for land cover while small fires are unequivocally selective (Nunes *et al.*,

2005). Larger fires are also detected in most fire prone regions of croplands in East China and grasslands in Inner Mongolia and West China.

Fire intensity defined by the 90th percentile of MODIS fire radiative power shows very high values in Northeast (Great Xing'an Mountains and Xiao Xing'an Mountains) and Southwest (Hengduan Mountains) China. Fire intensity and fire or burn severity have anecdotally been considered to be related, with more intense fires generally expected to cause more severe post-fire effects, and the 90th percentile of MODIS fire radiative power could be used to predict potential long-term negative ecological effects for individual fires (Heward *et al.*, 2013). Wooster *et al.* (2005) found that fire radiative energy (the temporal integral of FRP) and fuel mass combusted have a highly significant linear relationship, and FRP is well related to combustion rate.

Grassland fires with larger available fuel loads tend to have greater combustion completeness and release a greater proportion of their total theoretical heat yield (Wooster *et al.*, 2005), as in the case of grassland fires in Hengduan Mountains. In the case of forest fires (e.g. forest fires in Great Xing'an Mountains and Xiao Xing'an Mountains), the differences in dominant fire type would contribute to the differences in fire intensity and mean fuel consumption, which was found in the study of boreal forest fires in Russia and North America. North American fires have higher mean intensities, increasing in proportion to percentage tree cover, characteristics indicating likely crown fire dominance; Russian fires have lower mean intensities, independent of percentage tree cover, characteristics more indicative of surface fire activity (Wooster & Zhang, 2004).

Overall, environmental (vegetation, landscape, and climate) factors that help increase the amount of combustible materials and reduce the moisture of fuel loads will increase the combustion completeness, hence increase fire intensity. Low 90th percentile of FRP values in croplands probably resulted from the less amount of fuel mass comparing to other land cover types. However, high altitude and complex geomorphological characteristics may assist in increasing smoke plume heights and then contributing to the higher fire intensity (Martin *et al.*, 2010), as in the cases of Hengduan Mountains, Great Xing'an Mountains and Xiao Xing'an Mountains.

5.3 Cluster analysis of fire regimes

Cluster analysis was implemented to group the grid cells data based on principal components by using k-means algorithm, to achieve a better understanding in fire regimes in China. The estimation of fire regimes are influenced by many factors during the exploratory data process, including sample size, selected fire regime variables, chosen standardization method, and the selection of number of principal components and number of clusters. Also, different clustering algorithms and different criteria can be applied in order to measure how ‘close’ or ‘similar’ among the data. However, there is not a defined answer for ‘optimal’ solution in clustering. Consequently, the results of cluster analysis depends on certain specific choices of the user, nevertheless, the whole procedure can provide reliable results if the variability of its results are checked under different working conditions and its outcomes are critically interpreted in order to avoid physically meaningless results.

K-means clustering as the most popular non-hierarchical clustering technique has often been criticized due to the high likelihood of obtaining a locally optimal solution or because it is not directly derived from statistical distribution theory, however, it efficiently deals with high dimensional data and it has been found to recover true cluster structure well (Steinley, 2006, 2008). Several suggestions were provided to obtain more robust k-means results regarding to local optima issue: elaborating approaches for determining starting values; choosing solution that minimizes trace over the repeated runs; combining information regarding the cluster problem (number of clusters, number of variables, sample size, etc.) with the distribution of the local optima created from the multiple initializations to determine the quality of a cluster solution; a so-called ‘stability analysis’ that can identify the most stable solution and suggest the number of clusters and empirically derive cluster membership probabilities (Everitt *et al.*, 2011). An in depth of analysis of such strategies is out of the scope of this thesis. Instead, thanks to its simplicity, efficiency and more applicable in the variables which are measured in continuous scale and large number of grid cells, k-means clustering has been employed in this study to achieve a

reasonable and stable solution by using default algorithm in MATLAB (stated below).

The squared Euclidean distance measure, and the k-means++ algorithm for cluster center initialization (default algorithm in MATLAB), which was demonstrated that it achieves faster convergence to a lower sum of within-cluster, sum-of-squares point-to-cluster-centroid distances than Lloyd's algorithm (Arthur & Vassilvitskii, 2007), were used to yield cluster results close to optimal solutions. Several steps during the exploratory data process were followed to determine the quality and the robustness of the computed cluster solution. The method of variable normalization, which support that the variables are best explained by the components, was applied. Three methods of variable normalization were: standardizing by the range, z-score and standardizing by the maximum value. Although standardizing by the range was recommended to be the most effective method (Steinley, 2006), this method and standardizing by the maximum value both failed to provide the best solution for high proportion of variability extracted from the fire regime variables. Furthermore, consider a method to estimate number of clusters practically. Three types of methods: algorithmic methods, graphical methods, and formulaic methods, were discussed in Steinley (2006): the graphical methods, for example, a scree plot that shows the monotonic decreasing relationship between SSE and number of clusters, were least advocated because it is highly subjective. However, its simplicity is preferred, and the obtained results are in accordance with other considerations in the study. Finally, repeatedly run the clustering algorithm with different schemes combing standardization methods, number of principal components, and number of clusters, and determine a rational solution according to the overall performance. The results of first run of the determined scheme were retained.

The fire regimes results should not be expected as absolute and exclusive: indeed, the results of the cluster analysis procedure depends on the considered selection of fire regime variables. We postulate that all the variables selected in this study are meaningful and equivalently important, and the clustering results on the basis of these variables are reliable and comparable. Unavoidably, fire regime M based on the differences between burned area data and active fire data is limitedly

understood, and the more number of land cover variables added more weights on land cover variables which further helped differentiate fire regime B and G. In conclusion, the proposed fire regimes need to be interpreted critically given some uncertainty in remotely sensed data and cluster analysis.

5.4 Comparisons and implications of fire regimes

Detailed and valid field data on wildfire history are restrictedly accessible in China, and the use of remotely sensed data has become necessary in understanding fire regimes at national scale. Although certain separated data sources on forest and grassland fires and crop residue burning in the field are available in government-generated statistical data in province level, the discrepancy between statistics and satellite data can be remarkable, mostly because the statistical data is understated commonly due to some political and technical reasons (Yan *et al.*, 2006). Forest fire statistics was applied often in forest fire regime in some provinces but highly concentrated in Heilongjiang (Hu & Jin, 2002; Jin & Hu, 2002). Few studies were carried out on distribution characteristics and the influence factors of forest fires in China by using satellite data (Tian *et al.*, 2013). Krawchuk and Moritz (2009) has inferred historical fire regimes for China by quantifying the relationship between reference fire regime classes adopted by the LANDFIRE initiative in the United States and a global climate data set using generalized additive models. Comparing with previous studies, we expect to provide additional helpful information and a new different perspective to reveal fire regimes in China and support fire and land management decisions.

Despite the differences in temporal extent and context of the MODIS data and the modelled predictions in Krawchuk and Moritz (2009), similar fire regimes were mapped in both studies in western, northeastern and southwestern China (Table 6). Nevertheless, a 35-200-year return interval burning arid shrublands in western China contrasts relatively fire free regions in this study, and they also did not predict clear fire regimes in southeastern and southern China, where forest and savanna fires detected

by satellite data. These discrepancies are expected as the results of recent human activities, which accord with the forest fire studies in China showing anthropogenic ignition of forest fires is closely related to the residential distribution and the production mode (Liu *et al.*, 2012; Tian *et al.*, 2013). In a global perspective, remotely sensed fire regimes in China were typically characterized as low to medium fire activity, low variability and intensity, fairly small fires, and commonly with long duration (Chuvieco *et al.*, 2008; Archibald *et al.*, 2013), comparing with other fire active regions.

Table 6 Similarity in fire regimes between Krawchuk and Moritz (2009) and this study

Fire regimes in Krawchuk and Moritz (2009)	Fire regimes in this study	Location	Similarity
$R200+_{desert}$	Fire free	Western China	Mostly fire-free
$R0\text{-}35_{grass}$	Fire regime B	Northeastern China	Grassland fires, frequent
$R0\text{-}35_{forest}$	Fire regime G	Southwestern China	Forest fires, frequent
$R200+_{forest}$	Fire regime G	Southwestern China	Forest fires
$R35\text{-}200_{forest}$	Fire regime G	Northeastern China	Forest fires, less frequent

Although the relatively short-term archive of satellite data make it lack the information needed to gain an understanding of the long-term regime of fire in China's ecosystems, it still can continuously capture the current fire activity in regional and global scales, which should be valued more especially in China, because the recent fast socioeconomic development accompany with climate change might trigger dramatic changes included increased fire activity and the study of recent fire regimes could provide direct feedbacks for further natural resources management. Much higher fire activity in part of Northeast and East China in forest and lowlands highlighted in fire regime R, for example, could imply higher needs for forest fire prevention and developing sound fire management policy. The unknown fire regime M should be further investigated to have more comprehensive understanding on fire role in China's ecosystems.

6. Conclusions

This study reveals fire characteristics (i.e. fire frequency, burned area, variability, frequency-size inequality, seasonality and intensity) in China and discusses the possible drivers of their respective spatial distributions. Four fire regimes were further mapped on the basis of fire characteristics using a k-means clustering algorithm, which need to be interpreted critically given the influence factors of cluster analysis. The study aims to provide a new different perspective in understanding fire regime in China's ecological systems and further support in the decisions making of natural resources management.

The most fire prone areas (fire regime R) exist mainly in forests and lowlands in Northeast and East China with high fire frequency and area burned, and low inter-annual variability in cropland fires but relatively high inter-annual variability in forest fires, indicating different causes in fires (human caused vs lightning). The western China exhibits mostly fire free in areas adjacent to the Taklamakan Desert in the west of China, and where Inner Mongolia meets Mongolia at its western border in the central north of China. Small fires in central China, western China and part of Northeast China were undetectable in satellite burned area data and remain unclear in the fire regime (fire regime M). The relatively lower fire activity in the rest parts of China were clustered to two groups according to the similarity and vicinity of vegetation types, which show different inter-annual variation in fire frequency and annual area burned in different land cover types and regions. Inter-annual variability is mainly high in grassland fires but low in cropland fires (fire regime B). Forest fires show mainly high inter-annual variability in northern regions but low inter-annual variability in southern regions (fire regime G).

Fire season duration of forest fires is very long in southern and part of Southeast China (more than 9 months) but much shorter in southwestern China (less than 3 months) and very short in northeastern China (less than one month). Peak months of

fires occur in non-winter seasons in the north but in non-summer seasons in the south. Cropland fires last relatively long in northeastern China (less than 9 months) and mainly peak in spring (April) but short in eastern China (less than 6 months) and mostly peak in summer (June). Large fires can occur in all vegetation types, while larger and less frequent forest fires mostly happen in the north and in the south the forest fires are relatively small and more frequent. Fire intensity based on the 90th percentile of fire radiative power is very high in northern China (Great Xing'an and Xiao Xing'an Mountains) and southwestern China (Hengduan Mountains), but very low in lowlands in eastern and south-central China, which is possibly connected with the altitude. Most of fires are caused by human in China, and the spatial and temporal distribution of fire characteristics are the outcome of a long-term interaction of dominant drivers in fire regimes (vegetation, climate, and landscape) and the influence of human activity.

Further research on understanding the fire regime in central China and its possible main drivers is recommended in the background of recent changes in climatic and management conditions, even active fires in those regions may be considered insignificant previously. The potential topics to discuss include comparisons in mapping fire regimes by using active fire data and burned area data separately, or combing more remotely sensed datasets, correlation among fire regimes variables and influential ecological and anthropogenic factors, and expanding variables and algorithms in cluster analysis.

Acknowledgement

I would like to express my sincere gratitude to European Commission for providing me the Erasmus Mundus scholarship to finish this master study.

I highly appreciate my co-supervisor Prof. José M.C. Pereira for his excellent teaching on fire ecology and remote sensing, and his patience and kind supports during the whole process. I would like to thank my supervisor Dr. Francesco Pirotti for his great support in helping me to develop my background on spatial analysis, and creating the best research environment. I was very lucky to have the guidance on cluster analysis and MATLAB from Dr. Andrea Masiero, who has been incredibly supportive and responsive to answer my questions.

I own many thanks to Mr. Peng Lin who has greatly helped on all the programming languages I used in the study with his excellent knowledge and patience. I am very grateful for having the kind helps from Dr. Yannick Le Page when I have doubts in processing data and on knowledge about fire regimes.

I would like to thank my colleagues in the labs, Duarte Oom, Akli Benali, Ana Sá from Lisbon, and Marco Piragnolo, Paola Bonato, Fabrizio de Blasi from Padova, for their great company and helps on the study. I would also like to thank my friends from Erasmus programs, to name but a few, Cátia Traça, Vanessa Palma, and Ghenima Ghemouri for the supports on the topic and exams, and the wonderful time we have spent together in Europe.

References

Archibald, S. & Roy, D. (2009) Identifying individual fires from satellite-derived burned area data. *Geoscience and Remote Sensing Symposium, 2009 IEEE International, IGARSS 2009*, pp. III-160-III-163.

Archibald, S., Lehmann, C.E., Gómez-Dans, J.L. & Bradstock, R.A. (2013) Defining pyromes and global syndromes of fire regimes. *Proceedings of the National Academy of Sciences*, **110**, 6442-6447.

Archibald, S., Roy, D.P., Wilgen, V., Brian, W. & Scholes, R.J. (2009) What limits fire? An examination of drivers of burnt area in Southern Africa. *Global Change Biology*, **15**, 613-630.

Arthur, D. & Vassilvitskii, S. (2007) k-means++: The advantages of careful seeding. *Proceedings of the eighteenth annual ACM-SIAM symposium on Discrete algorithms*, pp. 1027-1035.

Barros, A.M. & Pereira, J.M. (2014) Wildfire selectivity for land cover type: does size matter? *PloS one*, **9**, e84760.

Bellù, L.G. & Liberati, P. (2006) Inequality analysis: the Gini index. *FAO, EASYPol Module*, **40**, 6-9.

Benali, A., Mota, B., Pereira, J., Oom, D. & Carvalhais, N. (2013) Global patterns of vegetation fire seasonality. *EGU General Assembly Conference Abstracts*, p. 11632.

Bowman, D.M., Balch, J.K., Artaxo, P., Bond, W.J., Carlson, J.M., Cochrane, M.A., D'Antonio, C.M., DeFries, R.S., Doyle, J.C. & Harrison, S.P. (2009) Fire in the Earth system. *science*, **324**, 481-484.

Calle, A., Sanz, J., Moclán, C., Romo, A. & Casanova, J. (2005) Detection and monitoring of forest fires in China through the ENVISAT-AATSR sensor. *Proceedings of the 5th International Workshop on Remote Sensing and GIS Applications to Forest Fire Management: Fire Effects Assessment*, pp. 16-18.

Chang, Y., He, H.S., Bishop, I., Hu, Y., Bu, R., Xu, C. & Li, X. (2007) Long-term forest landscape responses to fire exclusion in the Great Xing'an Mountains, China. *International Journal of Wildland Fire*, **16**, 34-44.

Chen, H., Hu, Y., Chang, Y., Bu, R., Li, Y. & Liu, M. (2011) Simulating impact of larch caterpillar (Dendrolimus superans) on fire regime and forest landscape in Da Hinggan Mountains, Northeast China. *Chinese Geographical Science*, **21**, 575-586.

Chuvieco, E. (2000) Remote sensing of forest fires. *Observing Land from Space: Science,*

Customers and Technology, pp. 47-51. Springer.

Chuvieco, E., Giglio, L. & Justice, C. (2008) Global characterization of fire activity: toward defining fire regimes from Earth observation data. *Global change biology*, **14**, 1488-1502.

Conedera, M., Tinner, W., Neff, C., Meurer, M., Dickens, A.F. & Krebs, P. (2009) Reconstructing past fire regimes: methods, applications, and relevance to fire management and conservation. *Quaternary Science Reviews*, **28**, 555-576.

Conover, W.J., Johnson, M.E. & Johnson, M.M. (1981) A comparative study of tests for homogeneity of variances, with applications to the outer continental shelf bidding data. *Technometrics*, **23**, 351-361.

Cumming, S. (2001) A parametric model of the fire-size distribution. *Canadian Journal of Forest Research*, **31**, 1297-1303.

Davies, G.M. (2013) Understanding Fire Regimes and the Ecological Effects of Fire. *Fire Phenomena and the Earth System*, pp. 95-124. John Wiley & Sons.

Everitt, B.S., Landau, S., Leese, M. & Stahl, D. (2011) Cluster Analysis. In, pp. 125-126. Wiley

Falk, D.A., Miller, C., McKenzie, D. & Black, A.E. (2007) Cross-scale analysis of fire regimes. *Ecosystems*, **10**, 809-823.

Falk, D.A., Heyerdahl, E.K., Brown, P.M., Farris, C., Fulé, P.Z., McKenzie, D., Swetnam, T.W., Taylor, A.H. & Van Horne, M.L. (2011) Multi-scale controls of historical forest-fire regimes: new insights from fire-scar networks. *Frontiers in Ecology and the Environment*, **9**, 446-454.

Fernandes, P.M. & Rigolot, E. (2007) The fire ecology and management of maritime pine (Pinus pinaster Ait.). *Forest Ecology and Management*, **241**, 1-13.

Flannigan, M., Campbell, I., Wotton, M., Carcaillet, C., Richard, P. & Bergeron, Y. (2001) Future fire in Canada's boreal forest: paleoecology results and general circulation model-regional climate model simulations. *Canadian Journal of Forest Research*, **31**, 854-864.

Fréjaville, T. & Curt, T. (2015) Spatiotemporal patterns of changes in fire regime and climate: defining the pyroclimates of south-eastern France (Mediterranean Basin). *Climatic Change*, **129**, 239-251.

Fulé, P.Z., Heinlein, T.A., Covington, W.W. & Moore, M.M. (2003) Assessing fire regimes on Grand Canyon landscapes with fire-scar and fire-record data. *International Journal of Wildland Fire*, **12**, 129-145.

Gavin, D.G., Hallett, D.J., Hu, F.S., Lertzman, K.P., Prichard, S.J., Brown, K.J., Lynch, J.A., Bartlein, P. & Peterson, D.L. (2007) Forest fire and climate change in western North America: insights from sediment charcoal records. *Frontiers in Ecology and the Environment*, **5**, 499-506.

Giglio, L., Descloitres, J., Justice, C.O. & Kaufman, Y.J. (2003) An enhanced contextual

fire detection algorithm for MODIS. *Remote sensing of environment*, **87**, 273-282.

Giglio, L., Loboda, T., Roy, D.P., Quayle, B. & Justice, C.O. (2009) An active-fire based burned area mapping algorithm for the MODIS sensor. *Remote Sensing of Environment*, **113**, 408-420.

Gill, J.L., Williams, J.W., Jackson, S.T., Lininger, K.B. & Robinson, G.S. (2009) Pleistocene megafaunal collapse, novel plant communities, and enhanced fire regimes in North America. *Science*, **326**, 1100-1103.

Gillett, N., Weaver, A., Zwiers, F. & Flannigan, M. (2004) Detecting the effect of climate change on Canadian forest fires. *Geophysical Research Letters*, **31**

Gundy, T.-V. & Melissa, A. (2014) Mapping fire regimes from data you may already have: assessing LANDFIRE fire regime maps using local products.

Guyette, R.P., Muzika, R.M. & Dey, D.C. (2002) Dynamics of an anthropogenic fire regime. *Ecosystems*, **5**, 472-486.

Guyette, R.P., Dey, D.C., Stambaugh, M.C. & Muzika, R.-M. (2005) Fire scars reveal variability and dynamics of eastern fire regimes. *Fire in eastern oak forests: delivering science to land managers, proceedings of a conference*, pp. 15-17.

Guyette, R.P., Stambaugh, M.C., Dey, D.C. & Muzika, R.-M. (2012) Predicting fire frequency with chemistry and climate. *Ecosystems*, **15**, 322-335.

He, C., Zhang, S.-Y., Chen, F. & Sun, Y. (2013) Forest fire division by using MODIS data based on the temporal-spatial variation law. *Spectroscopy and Spectral Analysis*, **33**, 2472-2477.

He, H.S., Shifley, S.R. & Thompson III, F.R. (2011) Overview of contemporary issues of forest research and management in China. *Environmental management*, **48**, 1061-1065.

Heward, H., Smith, A.M., Roy, D.P., Tinkham, W.T., Hoffman, C.M., Morgan, P. & Lannom, K.O. (2013) Is burn severity related to fire intensity? Observations from landscape scale remote sensing. *International journal of wildland fire*, **22**, 910-918.

Holden, Z., Smith, A., Morgan, P., Rollins, M. & Gessler, P. (2005) Evaluation of novel thermally enhanced spectral indices for mapping fire perimeters and comparisons with fire atlas data. *International Journal of Remote Sensing*, **26**, 4801-4808.

Hu, H. & Jin, S. (2002) Study on forest fire regime of Heilongjiang province II. Analysis on factors affecting fire dynamics and distributions. *Scientia Silvae Sinicae*, **38**, 98-102.

Huang, X., Li, M., Li, J. & Song, Y. (2012) A high-resolution emission inventory of crop burning in fields in China based on MODIS Thermal Anomalies/Fire products. *Atmospheric Environment*, **50**, 9-15.

Innes, J.L., Beniston, M. & Verstraete, M.M. (2000) *Biomass burning and its inter-relationships with the climate system*. Springer.

Jin, S. & Hu, H. (2002) Study on forest fire regime of Heilongjiang province I. Forest fire

spatial and temporal dynamics and statistical distribution. *Scientia Silvae Sinicae*, **38**, 88-94.

Kaiser, H.F. & Rice, J. (1974) Little Jiffy, Mark IV. *Educational and psychological measurement*, **34**, 111-117.

Kasischke, E.S. & Turetsky, M.R. (2006) Recent changes in the fire regime across the North American boreal region—spatial and temporal patterns of burning across Canada and Alaska. *Geophysical Research Letters*, **33**, L09703.

Knorr, W., Kaminski, T., Arneth, A. & Weber, U. (2014) Impact of human population density on fire frequency at the global scale. *Biogeosciences*, **11**, 1085-1102.

Krawchuk, M.A. & Moritz, M.A. (2009) Fire regimes of China: inference from statistical comparison with the United States. *Global Ecology and Biogeography*, **18**, 626-639.

Krebs, P., Pezzatti, G.B., Mazzoleni, S., Talbot, L.M. & Conedera, M. (2010) Fire regime: history and definition of a key concept in disturbance ecology. *Theory in Biosciences*, **129**, 53-69.

Le Page, Y., Oom, D., Silva, J., Jönsson, P. & Pereira, J. (2010) Seasonality of vegetation fires as modified by human action: observing the deviation from eco-climatic fire regimes. *Global Ecology and Biogeography*, **19**, 575-588.

Lehsten, V., Harmand, P., Palumbo, I. & Arneth, A. (2010) Modelling burned area in Africa. *Biogeosciences*, **7**, 3199-3214.

Lentile, L.B., Holden, Z.A., Smith, A.M., Falkowski, M.J., Hudak, A.T., Morgan, P., Lewis, S.A., Gessler, P.E. & Benson, N.C. (2006) Remote sensing techniques to assess active fire characteristics and post-fire effects. *International Journal of Wildland Fire*, **15**, 319-345.

Li, X., He, H.S., Wu, Z., Liang, Y. & Schneiderman, J.E. (2013) Comparing effects of climate warming, fire, and timber harvesting on a boreal forest landscape in Northeastern China. *PloS one*, **8**, e59747.

Liu, Z., Yang, J., Chang, Y., Weisberg, P.J. & He, H.S. (2012) Spatial patterns and drivers of fire occurrence and its future trend under climate change in a boreal forest of Northeast China. *Global Change Biology*, **18**, 2041-2056.

Lv, A.-F. (2011) Study on the relationship among forest fire, temperature and precipitation and its spatial-temporal variability in China. *Agricultural Science & Technology-Hunan*, **12**, 1396-1400.

Lynch, J.A., Hollis, J.L. & Hu, F.S. (2004) Climatic and landscape controls of the boreal forest fire regime: Holocene records from Alaska. *Journal of Ecology*, **92**, 477-489.

Malamud, B.D., Millington, J.D. & Perry, G.L. (2005) Characterizing wildfire regimes in the United States. *Proceedings of the National Academy of Sciences of the United States of America*, **102**, 4694-4699.

Mansuy, N., Boulanger, Y., Terrier, A., Gauthier, S., Robitaille, A. & Bergeron, Y. (2014)

Spatial attributes of fire regime in eastern Canada: influences of regional landscape physiography and climate. *Landscape ecology*, **29**, 1157-1170.

Marlon, J.R., Bartlein, P.J., Carcaillet, C., Gavin, D.G., Harrison, S.P., Higuera, P.E., Joos, F., Power, M. & Prentice, I. (2008) Climate and human influences on global biomass burning over the past two millennia. *Nature Geoscience*, **1**, 697-702.

Martin, M.V., Logan, J., Kahn, R., Leung, F., Nelson, D. & Diner, D. (2010) Smoke injection heights from fires in North America: analysis of 5 years of satellite observations. *Atmospheric Chemistry and Physics*, **10**, 1491-1510.

Molinario, G., Davies, D.K., Schroeder, W. & Justice, C.O. (2014) Characterizing the spatio-temporal fire regime in Ethiopia using the MODIS-active fire product: a replicable methodology for country-level fire reporting. *African Geographical Review*, **33**, 99-123.

Moreira, F., Viedma, O., Arianoutsou, M., Curt, T., Koutsias, N., Rigolot, E., Barbati, A., Corona, P., Vaz, P. & Xanthopoulos, G. (2011) Landscape–wildfire interactions in southern Europe: implications for landscape management. *Journal of environmental management*, **92**, 2389-2402.

Moreno, M.V. & Chuvieco, E. (2013) Characterising fire regimes in Spain from fire statistics. *International Journal of Wildland Fire*, **22**, 296-305.

Moreno, M.V., Conedera, M., Chuvieco, E. & Pezzatti, G.B. (2014) Fire regime changes and major driving forces in Spain from 1968 to 2010. *Environmental Science & Policy*, **37**, 11-22.

Morgan, P., Hardy, C.C., Swetnam, T.W., Rollins, M.G. & Long, D.G. (2001) Mapping fire regimes across time and space: understanding coarse and fine-scale fire patterns. *International Journal of Wildland Fire*, **10**, 329-342.

Niu, R. & Zhai, P. (2012) Study on forest fire danger over Northern China during the recent 50 years. *Climatic change*, **111**, 723-736.

Nunes, M.C., Vasconcelos, M.J., Pereira, J.M., Dasgupta, N., Alldredge, R.J. & Rego, F.C. (2005) Land cover type and fire in Portugal: do fires burn land cover selectively? *Landscape Ecology*, **20**, 661-673.

Oliveira, S.L., Pereira, J.M. & Carreiras, J.M. (2012) Fire frequency analysis in Portugal (1975–2005), using Landsat-based burnt area maps. *International Journal of Wildland Fire*, **21**, 48-60.

Oliveras, I., Anderson, L.O. & Malhi, Y. (2014) Application of remote sensing to understanding fire regimes and biomass burning emissions of the tropical Andes. *Global Biogeochemical Cycles*, **28**, 480-496.

Pausas, J.G. (2004) Changes in fire and climate in the eastern Iberian Peninsula (Mediterranean basin). *Climatic change*, **63**, 337-350.

Pausas, J.G. & Fernández-Muñoz, S. (2012) Fire regime changes in the Western Mediterranean Basin: from fuel-limited to drought-driven fire regime. *Climatic*

change, **110**, 215-226.

Pezzatti, G.B., Zumbrunnen, T., Bürgi, M., Ambrosetti, P. & Conedera, M. (2013) Fire regime shifts as a consequence of fire policy and socio-economic development: an analysis based on the change point approach. *Forest Policy and Economics*, **29**, 7-18.

Piñol, J., Beven, K. & Viegas, D.X. (2005) Modelling the effect of fire-exclusion and prescribed fire on wildfire size in Mediterranean ecosystems. *Ecological Modelling*, **183**, 397-409.

Rollins, M.G. (2009) LANDFIRE: a nationally consistent vegetation, wildland fire, and fuel assessment. *International Journal of Wildland Fire*, **18**, 235-249.

Rollins, M.G., Swetnam, T.W. & Morgan, P. (2001) Evaluating a century of fire patterns in two Rocky Mountain wilderness areas using digital fire atlases. *Canadian Journal of Forest Research*, **31**, 2107-2123.

Rollins, M.G., Keane, R.E. & Parsons, R.A. (2004) Mapping fuels and fire regimes using remote sensing, ecosystem simulation, and gradient modeling. *Ecological Applications*, **14**, 75-95.

Roy, D., Jin, Y., Lewis, P. & Justice, C. (2005) Prototyping a global algorithm for systematic fire-affected area mapping using MODIS time series data. *Remote sensing of environment*, **97**, 137-162.

Roy, D.P., Boschetti, L. & Smith, A. (2013) Satellite remote sensing of fires. *Fire Phenomena and the Earth System: An Interdisciplinary Guide to Fire Science*, 77-93.

Shapiro-Miller, L.B., Heyerdahl, E.K. & Morgan, P. (2007) Comparison of fire scars, fire atlases, and satellite data in the northwestern United States. *Canadian Journal of Forest Research*, **37**, 1933-1943.

Steinley, D. (2006) K-means clustering: a half-century synthesis. *British Journal of Mathematical and Statistical Psychology*, **59**, 1-34.

Steinley, D. (2008) Stability analysis in K-means clustering. *British Journal of Mathematical and Statistical Psychology*, **61**, 255-273.

Summers, W.T., Coloff, S.G. & Conard, S.G. (2011) Synthesis of Knowledge: Fire History and Climate Change.

Sun, L., Wang, Q., Wei, S., Hu, H., Guan, D. & Chen, X. (2014) Response characteristics and prospect of forest fire disasters in the context of climate change in China. *Journal of Catastrophology*, **1**, 003.

Tian, X.-R., Zhao, F.-J., Shu, L.-F., Miao, Q.-L. & Wang, M.-Y. (2014) Changes of climate and fire dynamic in China vegetation zone during 1961-2010. *The Journal of Applied Ecology*, **25**, 3279-3286.

Tian, X., Zhao, F., Shu, L. & Wang, M. (2013) Distribution characteristics and the influence factors of forest fires in China. *Forest Ecology and Management*, **310**, 460-467.

Wang, C., Gower, S.T., Wang, Y., Zhao, H., Yan, P. & Bond-Lamberty, B.P. (2001) The influence of fire on carbon distribution and net primary production of boreal Larix gmelinii forests in north-eastern China. *Global Change Biology*, **7**, 719-730.

Wang, X., He, H.S. & Li, X. (2007) The long-term effects of fire suppression and reforestation on a forest landscape in Northeastern China after a catastrophic wildfire. *Landscape and Urban Planning*, **79**, 84-95.

Wang, X., He, H.S., Li, X., Chang, Y., Hu, Y., Xu, C., Bu, R. & Xie, F. (2006) Simulating the effects of reforestation on a large catastrophic fire burned landscape in Northeastern China. *Forest Ecology and Management*, **225**, 82-93.

Whitlock, C., Higuera, P.E., McWethy, D.B. & Briles, C.E. (2010) Paleoecological perspectives on fire ecology: revisiting the fire-regime concept. *The Open Ecology Journal*, **3**, 6-23.

Wooster, M. & Zhang, Y. (2004) Boreal forest fires burn less intensely in Russia than in North America. *Geophysical Research Letters*, **31**, L20505.

Wooster, M.J., Roberts, G., Perry, G. & Kaufman, Y. (2005) Retrieval of biomass combustion rates and totals from fire radiative power observations: FRP derivation and calibration relationships between biomass consumption and fire radiative energy release. *Journal of Geophysical Research: Atmospheres (1984–2012)*, **110**, D24311.

Wu, Z.W., He, H.S., Chang, Y., Liu, Z.H. & Chen, H.W. (2011) Development of customized fire behavior fuel models for boreal forests of northeastern China. *Environmental management*, **48**, 1148-1157.

Yan, X., Ohara, T. & Akimoto, H. (2006) Bottom-up estimate of biomass burning in mainland China. *Atmospheric Environment*, **40**, 5262-5273.

Zhang, J.-H., Yao, F.-M., Liu, C., Yang, L.-M. & Boken, V.K. (2011) Detection, emission estimation and risk prediction of forest fires in China using satellite sensors and simulation models in the past three decades—An overview. *International journal of environmental research and public health*, **8**, 3156-3178.

Zumbrunnen, T., Menéndez, P., Bugmann, H., Conedera, M., Gimmi, U. & Bürgi, M. (2012) Human impacts on fire occurrence: a case study of hundred years of forest fires in a dry alpine valley in Switzerland. *Regional Environmental Change*, **12**, 935-949.